Appl. Comput. Math., V.22, N.2, 2023, pp.189-214
DOI: 10.30546/1683-6154.22.2.2023.189

A DELAYED ECO-EPIDEMIOLOGICAL COMPETITION NETWORK WITH REACTION-DIFFUSION TERMS: TIPPING ANTICIPATION

YUNXIANG LU[1], MIN XIAO[1,*], JIAJIN HE[1], XIANGYU DU[1]

Abstract. In order to better represent the behavioral variation and spatial crowding effect of competitors, a novel delayed eco-epidemiological competition network with diffusion effects is considered in this paper. The main objective is to investigate the Turing instability effected by diffusivity and determine the existence and properties of Hopf bifurcation. Through analyzing the corresponding characteristic equations, the Turing instability of the non-trivial equilibrium point and the existence of Hopf bifurcation are dissected. It is suggested that the abnormal diffusivity and the incubation period may lead to critical transitions in network dynamic behaviors such as the formation of diverse patterns delineated by amplitude maps and the appearance or disappearance of spatiotemporal oscillatory periodic solution. By virtue of the normal form theory and the center manifold reduction for reaction diffusion equations, qualities of the Hopf bifurcation are determined. Ultimately, to justify the correctness and effectiveness of theoretical results obtained, numerical simulations are demonstrated.

Keywords: Partial Differential Equation, Eco-Epidemiological Network, Tipping, Turing Instability, Hopf Bifurcation, Bifurcation Direction.

AMS Subject Classification: 16T05, 37L10, 37G15, 93C20.

1. Introduction

Numerous real-world complex networks are observed to go through sudden transitions in their patterns of behavior or dynamical states, and these phenomena are defined as tipping [2]. The tipping mechanism has been widely implemented in various scientific fields and in numerous applications [14, 22, 24, 25]. An interesting application is the utilization of tipping mechanism for constructing general purpose computing devices. The tipping points in complex systems are capable of switching between different attractors under small changes in one parameter, and this switching can be exploited to implement basic logic operations efficiently and flexibly [22]. Another interesting class of applications is in the detection of oscillatory instabilities in thermoacoustic systems. The inherent signal fluctuations induced by tipping points during stable system operation can be harnessed to provide early warning in real time, so that control actions can be initiated to mitigate the effects of critical transitions [24]. Thus, the search for early warning signals for such imminent critical transitions has become a focus of research [1, 26].

Epidemics seriously affect human life and safety [7]. Between 430 B.C. and 427 B.C., the outbreak of the plague devastated the Athenian civilization. The "Black Death" that broke out in the Middle Ages ravaged Europe, North Africa, the Middle East and parts of Asia, caused a quarter of Europe's population to drop sharply. The novel coronavirus disease 2019 (COVID-19) emerged at the end of 2019 and spread rapidly around the world [12]. The World Health Organization (WHO) had identified the new crown pneumonia epidemic as a "public health emergency of international concern" and had developed into a serious public health

[1]College of Automation and College of Artificial Intelligence, Nanjing University of Posts and Telecommunications, Nanjing 210003, China
e-mail: miraclemanlyx@163.com, ihejiajin@163.com, duxiangyv0617@163.com
[*]Corresponding author: e-mail: candymanxm2003@aliyun.com
Manuscript received 2 May 2022.

security problem affecting the world [5,11]. In a research report on "Threats of Avian Influenza Pandemic", the WHO clearly pointed out that epidemiological mathematical models have been regarded as a key factor in epidemic control and delayed transmission [32]. Thus, it is necessary and significant to explore epidemiological mathematical models theoretically and practically [6,12].

When it comes to the epidemiological model, it's natural to associate the ecological competition model. They complement and infiltrate each other, so that constitute an essential part of the ecosystem [10,19]. On account of the pioneering works on the predator-prey model in [20,29], the Lotka-Volterra models have set off an upsurge in the investigation of ecological competition networks [9, 18, 21, 33]. Previous studies have failed to demonstrate a correlation between epidemiological and ecological competition models due to being overly limited to the ecological competition model itself. Recent developments in the field of epidemiological models have led to a renewed interest in the area of eco-epidemiological competition networks [4, 16, 17, 31]. A mathematical model dealing with a predator-prey network with disease in the prey was proposed in [16]. The stability of the positive equilibrium was investigated and the properties of bifurcated periodic solutions were also determined through norm form theory and the center mainfold reduction. Motivated by this work, a delayed fractional eco-epidemiological network with incommensurate orders was suggested in [31]. It was indicated that the stability of the system can be optimized by the transformation of the feedback control delay. A novel delayed SIS eco-epidemiological competition network with different types of functional responses was established in [17]. It was observed that a Hopf bifurcation may occur around the equilibrium points when the incubation period passed through some critical values. Nevertheless, few of them considered the movement characteristics of species and mechanisms of virus transmission into the modeling of eco-epidemiological competitive networks, and researched the impact of such diffusion mechanisms governed by partial differential equations on evolutions of network dynamical behaviors. Therefore, considering the the movement of species and dispersal of epidemics in such eco-epidemiological competition model and exploring the spatiotemporal dynamical behaviors arising from such diffusion have great theoretical significance and practical requirements.

Partial differential equation is one of the fundamental equations describing natural diffusive phenomena. Reaction-diffusion networks delineated through partial differential equations have a wide range of applications in numerous fields such as physics, chemistry, biology, engineering, and so on [23,30]. A few but growing body of scholars started to investigate migration characteristics of species in eco-epidemiological competition network. In [28], the reaction-diffusion model of spread of influenza virus in both one and two dimensions was analyzed. It was demonstrated that diffusion has a significant effect on the spatial spread of epidemics. Chaotic waves appear to be a major mode of disease spread. This implies that influenza epidemics are bidirectional in transmission. A viral diseases propagation model with partly diffusive bacterial was explored in [27]. It was revealed that chemotaxis may cause the Turing bifurcations and the model has no Turing bifurcations when the chemotaxis disappear. The formation of spatial pattern in a diffusive predator-prey-parasite (PPP) model was addressed in [8], and it was found that instability driven by diffusion creates diverse variety of spatiotemporal patterns, like spot, stripe, mixture of spots & stripes and spiral patterns, depending upon the values of diffusion and ecological parameters. However, delays such as the incubation period of epidemics are not considered in the systematic modeling of these literatures. It is well-known that the incubation period delay is an momentous parameter of the epidemic model, and its increase or decrease will cause huge distortions to dynamic behaviors of the network, such as bifurcation or even chaos [3, 10, 34]. A diffusive epidemic model with two delays subjecting to the Neumann boundary conditions was considered in [10], and the normal form on the center manifold near the Hopf bifurcation singularity was derived. A time-periodic two-strain SIS epidemic model with diffusion and latent period was investigated in [34]. The basic reproduction number and the invasion number which can evaluate the ability of each strain to invade the other single-strain were determined,

respectively. Although these models considered ecological competition networks with disease and delay, they had not been able to reasonably describe the transmission mechanism of the virus. Most of them employed disease transmission mechanisms with the bilinear incidence rate $\beta S(t)I(t)$ and the standard incidence rate $(\beta S(t)I(t))/(S(t)+I(t)+R(t))$. Both of these two incidences have certain limitations, under which the infected species grow linearly. It is completely different from the actual situation [19].

In order to better represent the behavioural variation and spatial crowding effect of competitors, the nonlinear saturated incidence rate mechanism and the incubation period delay of the epidemic should be considered in eco-epidemiological competition networks, simultaneously. A powerful early warning signal which is rooted in the Hopf bifurcation was introduced in [14] to anticipate and distinguish the coming tipping. It was demonstrated that the spatial self-organization induced by the Turing instability in ecosystems is a prominent early warning signal in [25]. Therefore, both the Hopf bifurcation theory and the Turing instability theory should be applied to make early anticipations of tipping points in the eco-epidemic network from two perspectives. To the best of the authors' knowledge, such the Turing instability governed by diffusive factors and the Hopf bifurcation induced by incubation period delay obstacles have never been investigated, synchronously. As a consequence, a delayed eco-epidemiological competition network with diffusion effects described by second order partial differential equation and nonlinear saturation incidence rate is proposed for the first time in this paper. Then, the stability of the non-trivial equilibrium point and the formation of spatiotemporal patterns on the spread of infected weak competitors processing nonlinear saturation incidence rate underneath the Neumann boundary conditions are determined, respectively. The oneset of incubation period defined as the Hopf bifurcation parameter is also derived. Furthermore, the properties of the Hopf bifurcation are qualified, such as the directions, the stability and the period of the bifurcating periodic solutions.

The organization of the paper is as follows. A novel delayed eco-epidemiological competition network with diffusion effects described by second order linear partial differential equation and nonlinear saturation incidence rate is put forward in Section 2. In Section 3, conditions of the Turing stability without time delay and the Hopf bifurcation derived by the incubation period are provided, respectively. Section 4 is dedicated to determine the qualities of the Hopf bifurcation. To verify the theoretical results, numerical simulations are carried out in Section 5. Finally, the paper is accomplished through conclusion presented in Section 6.

2. The description of a delayed eco-epidemiological competition network

Motivated by these previous works [4, 10, 19, 31, 34], a delayed eco-epidemiological network with reaction diffusion terms and nonlinear saturation incidence rate is investigate as follows

$$\begin{cases} \frac{\partial S(x,t)}{\partial t} = d_1\Delta S(x,t) + aS(x,t)(1-\frac{S(x,t)+I(x,t)}{K}) - \frac{\beta S(x,t)I(x,t-\tau)}{1+\alpha I(x,t-\tau)} - p_1S(x,t)Y(x,t), \\ \frac{\partial I(x,t)}{\partial t} = d_2\Delta I(x,t) + \frac{\beta S(x,t)I(x,t-\tau)}{1+\alpha I(x,t-\tau)} - p_2I(x,t)Y(x,t) - cI(x,t), \\ \frac{\partial Y(x,t)}{\partial t} = d_3\Delta Y(x,t) + qp_1S(x,t)Y(x,t) + qp_2I(x,t)Y(x,t) - dY(x,t), \\ x\in\Omega,\ t>0, \end{cases} \tag{1}$$

under the Neumann boundary conditions

$$\frac{\partial S(x,t)}{\partial x} = \frac{\partial I(x,t)}{\partial x} = \frac{\partial Y(x,t)}{\partial x} = 0,\ x=\partial\Omega,\ t>0,$$

with the initial conditions

$$S(x,t) = S_0(x,t) \geq 0, I(x,t) = I_0(x,t) \geq 0, Y(x,t) = Y_0(x,t) \geq 0, x\in\bar{\Omega},\ t\in[-\tau,0],$$

in which $S(x,t)$, $I(x,t)$, and $Y(x,t)$ denote the population of susceptible weak competitor, infected weak competitor and strong competitor at location x and time t, respectively. d_1, d_2 and d_3 stand for the diffusive coefficients of susceptible weak competitor, infected weak competitor and strong competitor, severally. $\beta S(x,t)I(x,t)/(1+\alpha I(x,t))$ represents nonlinear saturation incidence rate among weak competitor. $\Omega = (0, l\pi)\,(l > 0)$ is the one-dimensional spatial domain with smooth boundary $\partial\Omega$, $\Delta = \partial^2/\partial x^2$. The Neumann (zero-flux) boundary conditions indicate that the domain boundary is insulated by default, and domain is isolated from the external environment, i.e., the habitat is encompassed by diffusive epidemic so that competitors can not leave the domain Ω and competitors that are outside the domain can not enter. The rest of the parameters are enumerated in Table 1.

Remark 1. *Compared with the previous works [4,10,19,31,34], there are two primary differences in this paper. One difference lies in the selection of the form of the differential equation adopted for the inscription of the network. A number of traditional ecological networks are portrayed by integer-order or fractional-order differential equations, which ignore the movement characteristics and cross-interference of competitors [19, 31]. For this reason, the second order partial differential equation is attempted to describe the diffusion phenomenon of competitors. The other difference is the selection of the form of the epidemic incidence. In contrast to the traditional bilinear incidence and standard incidence, the nonlinear saturation incidence appears to be a more reasonable description of disease transmission within the network. It includes the behavioural variations and crowding effect of the infective individuals, and prevents the unboundedness of the contact rate by choosing suitable parameters [4, 10, 34].*

Table 1. The definitions of parameters in network (1).

Symbol	Parameter definition
K	The environment carrying capacity for weak competitor
a	The intrinsic growth rate of susceptible weak competitor
c	The natural death rate of infected weak competitor
d	The natural death rate of strong competitor
α	The prevention coefficient of epidemic
β	The infection coefficient of epidemic
p_1	The coefficient of predation for susceptible weak competitor to strong competitor
p_2	The coefficient of predation for infected weak competitor to strong competitor
q	The coefficient of conversing weak competitor to strong competitor
τ	The incubation period delay of the epidemic in weak competitor

To establish our main results, the following hypothesis are needed

$$(H_1)\ (B^2 - 4AC)^{\frac{1}{2}} \le B,\ d \ge qp_1S^*,\ \frac{\beta S^*}{1+\alpha I^*} \ge c,$$

where

$$\begin{aligned} A &= a\alpha p_1 q^2(p_1 - p_2) < 0, \\ B &= (ap_2^2 - ap_1p_2 + \alpha cKp_1^2 + a\alpha Kp_1p_2)q^2 + (dp_2 - 2dp_1)a\alpha q, \\ C &= -(ap_2 + cp_1)Kp_2q^2 + [(a + \beta K - a\alpha K)p_2 - \alpha cKp_1]dq + a\alpha d^2. \end{aligned}$$

Remark 2. *p_1 and p_2 denote predation coefficients of susceptible weak competitor and infected weak competitor to strong competitor. The health of the infected weak competitor is out of condition. It is obvious that $p_1 < p_2$ due to the principle of survival of the best in nature, so that the predation rate of the infected weak competitor by strong competitors is greatly increased.*

Under the hypothesis (H_1), it is calculated that the non-trivial equilibrium point $E^*(S^*, I^*, Y^*)$ of network (1) is defined by

$$S^* = \frac{-B + \sqrt{B^2 - 4AC}}{2A},$$
$$I^* = \frac{d - qp_1S^*}{qp_2},$$
$$Y^* = \frac{1}{p_2}(\frac{\beta S^*}{1 + \alpha I^*} - c).$$

Remark 3. *The above hypothesis is made to ensure that there must be a non-trivial equilibrium point in network (1), which makes the research meaningful. Therefore, the whole text is based on this assumption. An example of the meaningful coexistence state of the susceptible weak competitor population, infected weak competitor population, and strong competitor population is presented in Fig.1, where* $a = 0.6,\ K = 1,\ p_1 = 0.125,\ p_2 = 6,\ c = 0.25,\ q = 0.75,\ d = 0.5,\ \alpha = 0.5,\ \beta = 0.7.$

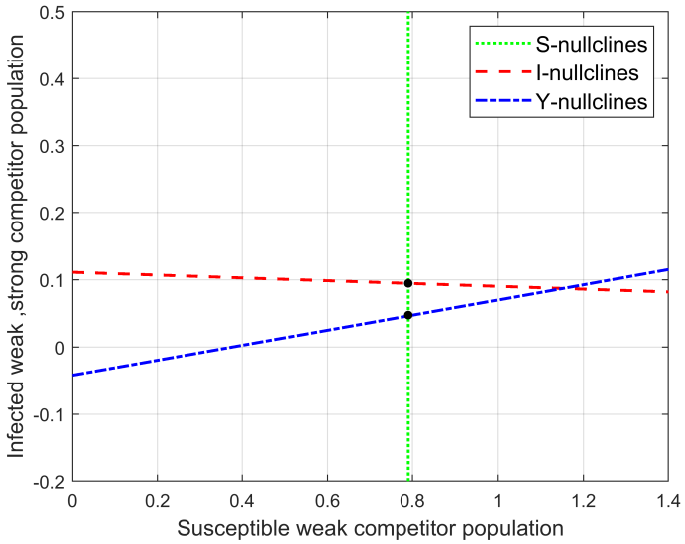


Figure 1. Graphs of S-nullcline (green), I-nullcline (red), and Y-nullcline (blue) for network (1) with $a = 0.6,\ K = 1,\ p_1 = 0.125,\ p_2 = 6,\ c = 0.25,\ q = 0.75,\ d = 0.5,\ \alpha = 0.5,\ \beta = 0.7$. There exists a non-trivial equilibrium point $E^*(0.7903, 0.0946, 0.0464)$.

Let $\tilde{S}(t) = S(t) - S^*$, $\tilde{I}(t) = I(t) - I^*$, $\tilde{Y}(t) = Y(t) - Y^*$. Dropping the tildes '$\sim$', then network (1) becomes

$$\begin{cases} \frac{\partial S(x,t)}{\partial t} = d_1\Delta S(x,t) + a_{11}S(x,t) + a_{12}I(x,t) + b_{12}I(x,t-\tau) + a_{13}Y(x,t) + f_1, \\ \frac{\partial I(x,t)}{\partial t} = d_2\Delta I(x,t) + a_{21}S(x,t) + a_{22}I(x,t) + b_{22}I(x,t-\tau) + a_{23}Y(x,t) + f_2, \\ \frac{\partial Y(x,t)}{\partial t} = d_3\Delta Y(x,t) + a_{31}S(x,t) + a_{32}I(x,t) + a_{33}Y(x,t) + f_3, \end{cases} \tag{2}$$

where

$$a_{11} = a - \frac{2a}{K}S^* - \frac{a}{K}I^* - \frac{\beta I^*}{1 + \alpha I^*} - p_1Y^*,\ a_{12} = -\frac{a}{K}S^*,\ b_{12} = -\frac{\beta S^*}{(1 + \alpha I^*)^2},$$
$$a_{13} = -p_1S^*,\ a_{21} = \frac{\beta I^*}{1 + \alpha I^*},\ a_{22} = -p_2Y^* - c,\ b_{22} = \frac{\beta S^*}{(1 + \alpha I^*)^2},$$
$$a_{23} = -p_2I^*,\ a_{31} = qp_1Y^*,\ a_{32} = qp_2Y^*,\ a_{33} = qp_1S^* + qp_2I^* - d,$$

and

$$\begin{aligned}
f_1 =& a_{14}S^2(x,t) + a_{15}S(x,t)I(x,t) + a_{16}S(x,t)Y(x,t) + b_{13}S(x,t)I(x,t-\tau) \\
&+ b_{14}I^2(x,t-\tau) + b_{15}S(x,t)I^2(x,t-\tau) + b_{16}I^3(x,t-\tau), \\
f_2 =& a_{24}I(x,t)Y(x,t) + b_{23}S(x,t)I(x,t-\tau) + b_{24}I^2(x,t-\tau) \\
&+ b_{25}S(x,t)I^2(x,t-\tau) + b_{26}I^3(x,t-\tau), \\
f_3 =& a_{34}S(x,t)Y(x,t) + a_{35}I(x,t)Y(x,t),
\end{aligned}$$

with

$$\begin{aligned}
&a_{14} = -\frac{a}{K},\ a_{15} = -\frac{a}{K},\ a_{16} = -p_1,\ b_{13} = -\frac{\beta}{(1+\alpha I^*)^2},\ b_{14} = \frac{\alpha\beta S^*}{(1+\alpha I^*)^3}, \\
&b_{15} = \frac{\alpha\beta}{(1+\alpha I^*)^3},\ b_{16} = -\frac{\alpha^2\beta S^*}{(1+\alpha I^*)^4},\ a_{24} = -p_2,\ b_{23} = \frac{\beta}{(1+\alpha I^*)^2}, \\
&b_{24} = -\frac{\alpha\beta S^*}{(1+\alpha I^*)^3},\ b_{25} = -\frac{\alpha\beta}{(1+\alpha I^*)^3},\ b_{26} = \frac{\alpha^2\beta S^*}{(1+\alpha I^*)^4},\ a_{34} = qp_1,\ a_{35} = qp_2.
\end{aligned}$$

Thus, the linear formation of network (2) is

$$\begin{cases}
\frac{\partial S(x,t)}{\partial t} = d_1\Delta S(x,t) + a_{11}S(x,t) + a_{12}I(x,t) + b_{12}I(x,t-\tau) + a_{13}Y(x,t), \\
\frac{\partial I(x,t)}{\partial t} = d_2\Delta I(x,t) + a_{21}S(x,t) + a_{22}I(x,t) + b_{22}I(x,t-\tau) + a_{23}Y(x,t), \\
\frac{\partial Y(x,t)}{\partial t} = d_3\Delta Y(x,t) + a_{31}S(x,t) + a_{32}I(x,t) + a_{33}Y(x,t).
\end{cases} \tag{3}$$

Separating the state variables with and without time delays, the equations given in (3) can be rewritten as

$$\frac{\partial}{\partial t}\begin{pmatrix} S(x,t) \\ I(x,t) \\ Y(x,t) \end{pmatrix} = (D\Delta + M)\begin{pmatrix} S(x,t) \\ I(x,t) \\ Y(x,t) \end{pmatrix} + N\begin{pmatrix} S(x,t-\tau) \\ I(x,t-\tau) \\ Y(x,t-\tau) \end{pmatrix}, \tag{4}$$

where

$$D = \begin{pmatrix} d_1 & 0 & 0 \\ 0 & d_2 & 0 \\ 0 & 0 & d_3 \end{pmatrix}, M = \begin{pmatrix} a_{11} & a_{12} & a_{13} \\ a_{21} & a_{22} & a_{23} \\ a_{31} & a_{32} & a_{33} \end{pmatrix}, N = \begin{pmatrix} 0 & b_{12} & 0 \\ 0 & b_{22} & 0 \\ 0 & 0 & 0 \end{pmatrix}.$$

Define $-k^2$ ($k \in \mathrm{N}_0$) to be the eigenvalue of the Laplacian operator Δ on Ω under homogeneous the Neumann boundary conditions, and the characteristic equations of network (4) are given by $\det(\lambda I_{3\times3} - \kappa_k - M - Ne^{-\lambda\tau}) = 0$, where $I_{3\times3}$ is a 3×3 identity matrix, $\kappa_k = -k^2D$. Since

$$\det(\lambda I_{3\times3} - \kappa_k - M - Ne^{-\lambda\tau}) = \begin{vmatrix} \lambda + d_1k^2 - a_{11} & -a_{12} - b_{12}e^{-\lambda\tau} & -a_{13} \\ -a_{21} & \lambda + d_2k^2 - a_{22} - b_{22}e^{-\lambda\tau} & -a_{23} \\ -a_{31} & -a_{32} & \lambda + d_3k^2 - a_{33} \end{vmatrix},$$

then, the characteristic equation of network (4) is

$$\lambda^3 + A_0(k^2)\lambda^2 + A_1(k^2)\lambda + A_2(k^2) + [A_3(k^2)\lambda^2 + A_4(k^2)\lambda + A_5(k^2)]e^{-\lambda\tau} = 0, \tag{5}$$

where

$$
\begin{aligned}
&A_0(k^2) = \phi_0 k^2 + \phi_1,\ A_1(k^2) = \phi_2 k^4 + \phi_3 k^2 + \phi_4,\\
&A_2(k^2) = \phi_5 k^6 + \phi_6 k^4 + \phi_7 k^2 + \phi_8,\ A_3(k^2) = \phi_9,\\
&A_4(k^2) = \phi_{10} k^2 + \phi_{11},\ A_5(k^2) = \phi_{12} k^4 + \phi_{13} k^2 + \phi_{14},\\
&\phi_0 = d_1 + d_2 + d_3,\ \phi_1 = -a_{11} - a_{22} - a_{33},\ \phi_2 = d_1 d_2 + d_1 d_3 + d_2 d_3,\\
&\phi_3 = -a_{11} d_2 - a_{11} d_3 - a_{22} d_1 - a_{22} d_3 - a_{33} d_1 - a_{33} d_2,\\
&\phi_4 = a_{11} a_{22} - a_{12} a_{21} + a_{11} a_{33} - a_{13} a_{31} + a_{22} a_{33} - a_{23} a_{32},\\
&\phi_5 = d_1 d_2 d_3,\ \phi_6 = -a_{11} d_2 d_3 - a_{22} d_1 d_3 - a_{33} d_1 d_2,\\
&\phi_7 = a_{11} a_{22} d_3 - a_{12} a_{21} d_3 + a_{11} a_{33} d_2 - a_{13} a_{31} d_2 + a_{22} a_{33} d_1 - a_{23} a_{32} d_1,\\
&\phi_8 = a_{11} a_{23} a_{32} - a_{11} a_{22} a_{33} + a_{12} a_{21} a_{33} - a_{12} a_{23} a_{31} - a_{13} a_{21} a_{32} + a_{13} a_{22} a_{31},\\
&\phi_9 = -b_{22},\ \phi_{10} = -b_{22} d_1 - b_{22} d_3,\ \phi_{11} = a_{11} b_{22} - a_{21} b_{12} + a_{33} b_{22},\\
&\phi_{12} = -b_{22} d_1 d_3,\ \phi_{13} = a_{11} b_{22} d_3 + a_{33} b_{22} d_1 - a_{21} b_{12} d_3,\\
&\phi_{14} = -a_{11} a_{33} b_{22} + a_{21} a_{33} b_{12} + a_{13} a_{31} b_{22} - a_{23} a_{31} b_{12}.
\end{aligned}
$$

3. Analysis of the Turing instability and the Hopf bifurcation

In this section, we seek for the conditions of the Turing instability on the approach of the characteristic equation for network (1) when $\tau = 0$. In addition, the criteria of the Hopf bifurcation for network (1) by adopting time delay as the bifurcation parameter are also revealed.

3.1. **The Turing instability analysis induced by diffusion.** In this subsection, we analyze the Turing instability of network (1) with no delay. When $\tau = 0,\ d_i = 0\ (i = 1, 2, 3)$, the characteristic equation of network (4) is simplified to

$$\lambda^3 + \varphi_0 \lambda^2 + \varphi_1 \lambda + \varphi_2 = 0, \tag{6}$$

where

$$
\begin{aligned}
\varphi_0 =& -a_{11} - a_{22} - a_{33} - b_{22},\\
\varphi_1 =& a_{11} a_{22} - a_{12} a_{21} + a_{11} a_{33} - a_{13} a_{31} + a_{22} a_{33}\\
&- a_{23} a_{32} + a_{11} b_{22} - a_{21} b_{12} + a_{33} b_{22},\\
\varphi_2 =& -a_{11} a_{22} a_{33} + a_{11} a_{23} a_{32} + a_{12} a_{21} a_{33} - a_{12} a_{23} a_{31} - a_{13} a_{21} a_{32}\\
&+ a_{13} a_{22} a_{31} - a_{11} a_{33} b_{22} + a_{13} a_{31} b_{22} + a_{21} a_{33} b_{12} - a_{23} a_{31} b_{12}.
\end{aligned}
$$

We make the following hypothesis

$$(H_2)\ \varphi_0 > 0,\ \varphi_1 > 0,\ \varphi_2 > 0,\ \varphi_0 \varphi_1 > \varphi_2.$$

Lemma 1. *Let us consider the network (1) with $\tau = 0,\ d_i = 0\ (i = 1, 2, 3)$. If (H_1) and (H_2) are satisfied, then the non-trivial equilibrium point $E^*(S^*, I^*, Y^*)$ is locally asymptotically stable.*

Remark 4. *It is apparent by the Routh-Hurwitz criterion that all roots of (6) will have negative real parts if (H_2) is arrived. Therefore, the proof is omitted here. As illustrated in Fig.2, when coefficients of network (1) satisfy (H_1) and (H_2), solutions approach the meaningful non-trivial equilibrium point $E^*(S^*, I^*, Y^*)$, gradually.*

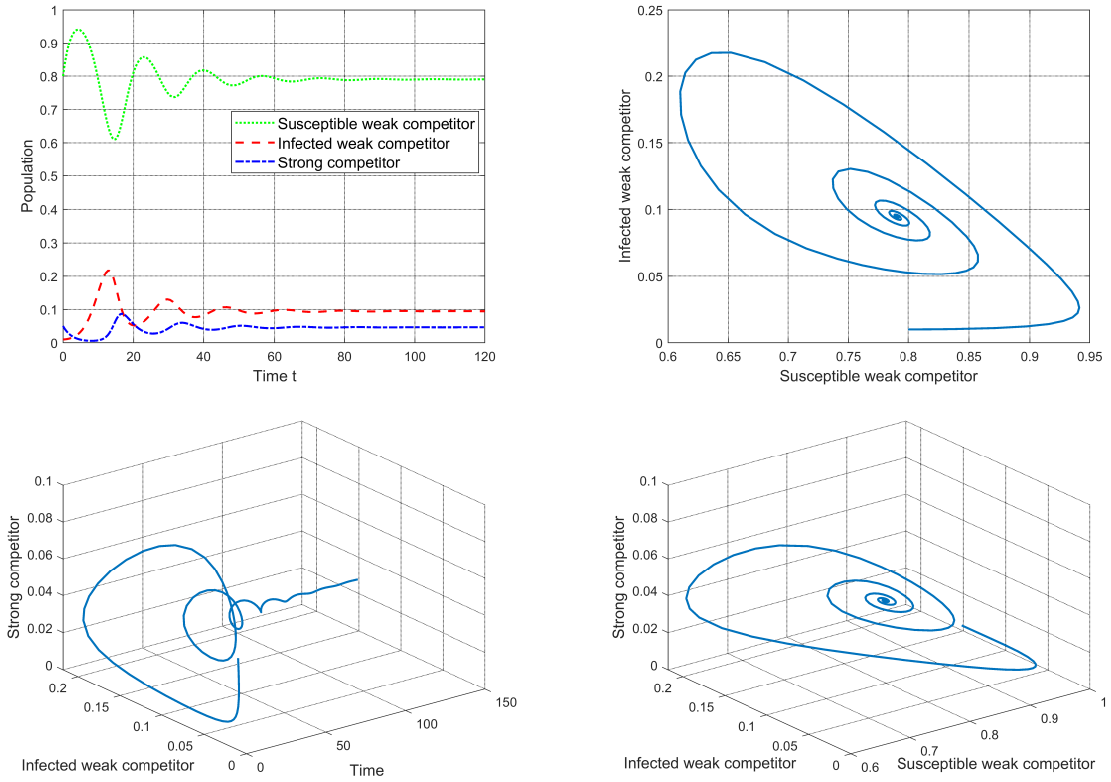


Figure 2. Waveform plots and portrait diagrams of network (1) satisfying (H_1) and (H_2), and the initial condition is $(0.8, 0.01, 0.05)$. The meaningful non-trivial equilibrium point $E^*(0.7903, 0.0946, 0.0464)$ is locally asymptotically stable. The parameter values are
$a = 0.6,\ k = 1,\ p_1 = 0.125,\ p_2 = 6,\ c = 0.25,\ q = 0.75,\ d = 0.5,\ \alpha = 0.5,\ \beta = 0.7.$

When $\tau = 0,\ d_i \neq 0\ (i = 1, 2, 3)$, the characteristic equation of network (4) is transformed into

$$\lambda^3 + B_0(k^2)\lambda^2 + B_1(k^2)\lambda + B_2(k^2) = 0, \tag{7}$$

in which

$$\begin{aligned}
&B_0(k^2) = B_{01}k^2 + \varphi_0,\ B_1(k^2) = B_{11}k^4 + B_{12}k^2 + \varphi_1,\\
&B_2(k^2) = B_{21}k^6 + B_{22}k^4 + B_{23}k^2 + \varphi_2,\\
&B_{01} = d_1 + d_2 + d_3,\ B_{11} = d_1d_2 + d_1d_3 + d_2d_3,\\
&B_{12} = (-b_{22} - a_{22})(d_1 + d_3) - a_{11}(d_2 + d_3) - a_{33}(d_1 + d_2),\\
&B_{21} = d_1d_2d_3,\ B_{22} = -a_{33}d_1d_2 - (a_{22} + b_{22})d_1d_3 - a_{11}d_2d_3,\\
&B_{23} = (a_{22}a_{33} - a_{23}a_{32} + a_{33}b_{22})d_1 + (a_{11}a_{33} - a_{13}a_{31})d_2\\
&\qquad + (a_{11}a_{22} - a_{12}a_{21} + a_{11}b_{22} - a_{21}b_{12})d_3.
\end{aligned}$$

To establish the Turing instability of network (1) with $\tau = 0,\ d_i \neq 0\ (i = 1, 2, 3)$, let

$$\begin{aligned}
&G(k^2) = B_{01}k^2 + \varphi_0,\\
&H(k^2) = B_{11}(k^2)^2 + B_{12}k^2 + \varphi_1,\\
&I(k^2) = B_{21}(k^2)^3 + B_{22}(k^2)^2 + B_{23}k^2 + \varphi_2,
\end{aligned}$$

and we address the following hypotheses

(H_3) $B_{01} < 0$ or $B_{11} < 0$ or $B_{21} < 0$;

(H_4) $B_{11} > 0,\ B_{12} < 0, B_{12}^2 - 4B_{11}\varphi_1 > 0,$

$$\lfloor\sqrt{s_2}\rfloor - \lceil\sqrt{s_1}\rceil \geq 0, \text{ in which } s_{1,2} = \frac{-B_{12} \pm \sqrt{B_{12}^2 - 4B_{11}\varphi_1}}{2B_{11}};$$

(H_5) $B_{21} > 0, B_{23} < 0,\ I(\lfloor\sqrt{x_+}\rfloor) < 0$ or $I(\lceil\sqrt{x_+}\rceil) < 0,$

$$\text{in which } x_+ = \frac{-B_{22} + \sqrt{B_{22}^2 - 3B_{21}B_{23}}}{3B_{21}}.$$

Lemma 2. *Suppose that (H_2) is respected.*

1) *If $B_{01} < 0$ is satisfied, there exists at least one positive integer $k_0 \in \left(\sqrt{-\varphi_0/B_{01}}, +\infty\right)$ such that $G(k_0^2) < 0$.*
2) *If $B_{11} < 0$ is satisfied, there exists at least one positive integer $k_1 \in \left(\sqrt{s_2}, +\infty\right)$ such that $H(k_1^2) < 0$.*
3) *If $B_{21} < 0$ is satisfied, there exists at least one positive integer $k_2 \in \left(\sqrt{x_+}, +\infty\right)$ such that $I(k_2^2) < 0$.*

Proof. On account of $\varphi_0 > 0$ and $B_{01} < 0$, we obtain that $G(0) = \varphi_0 > 0$, $\lim\limits_{k\to+\infty} G(k^2) = -\infty$ and $G(k^2)$ is a monotonically decreasing function of k^2 whose intersection with the positive horizontal semi-axis is $\sqrt{-\varphi_0/B_{01}}$. It is apparent that there must be a positive integer $k_0 \in \left(\sqrt{-\varphi_0/B_{01}}, +\infty\right)$ such that $G(k_0^2) < 0$. This completes the proof of 1). 2) and 3) can also be proved by the same method, so that the detailed proof will not be provided here. □

Lemma 3. *If (H_2) and (H_4) are satisfied, there exists at least one positive integer $k_3 \in \left(\sqrt{s_1}, \sqrt{s_2}\right)$ such that $H(k_3^2) < 0$.*

Proof. Define $s\ (> 0) = k^2$, we achieve

$$H(s) = B_{11}s^2 + B_{12}s + \varphi_1.$$

According to hypotheses $B_{11} > 0,\ B_{12} < 0, B_{12}^2 - 4B_{11}\varphi_1 > 0, \varphi_1 > 0$, $H(s)$ is a quadratic parabolic function with an upward opening. $H(s) = 0$ has two positive real roots, which are $s_{1,2} = (-B_{12} \pm \sqrt{B_{12}^2 - 4B_{11}\varphi_1})\Big/2B_{11}$. It is less difficult to know that $H(s) < 0$ while $s \in (s_1, s_2)$. Since $s = k^2$, $H(k^2) < 0$ then $k \in \left(\sqrt{s_1}, \sqrt{s_2}\right)$. Based on the rounding function inequality $\lfloor\sqrt{s_2}\rfloor - \lceil\sqrt{s_1}\rceil \geq 0$, restricting at least one positive integer between $\sqrt{s_1}$ and $\sqrt{s_2}$, it is obvious that there exists at least one positive integer $k_3 \in \left(\sqrt{s_1}, \sqrt{s_2}\right)$ such that $H(k_3^2) < 0$. This proof is accomplished. □

Lemma 4. *If (H_2) and (H_5) are satisfied, there exists at least one positive integer $k_4 = \lfloor\sqrt{x_+}\rfloor$ or $\lceil\sqrt{x_+}\rceil$ such that $I(k_4^2) < 0$.*

Proof. Define $x\ (> 0) = k^2$, we get

$$I(x) = B_{21}x^3 + B_{22}x^2 + B_{23}x + \varphi_2.$$

Since $B_{21} > 0$ and $B_{23} < 0$, we calculate that $I'(x) = 3B_{21}x^2 + 2B_{22}x + B_{23} = 0$ has two roots $x_- = (-B_{22} - \sqrt{B_{22}^2 - 3B_{21}B_{23}})\Big/(3B_{21}) < 0$ and $x_+ = (-B_{22} + \sqrt{B_{22}^2 - 3B_{21}B_{23}})\Big/(3B_{21}) > 0$. According to the extreme value theorem of the univariate cubic equation $I''(x_-) < 0$ and $I''(x_+) > 0$, $I(x)$ will obtain the local maximum and local minimum points at x_- and x_+, respectively. As $I(\lfloor\sqrt{x_+}\rfloor) < 0$ or $I(\lceil\sqrt{x_+}\rceil) < 0$, it's not intricate for us to get that there exists at least one positive integer $k_4 = \lfloor\sqrt{x_+}\rfloor$ or $\lceil\sqrt{x_+}\rceil$ such that $I(k_4^2) < 0$. This ends the proof. □

Theorem 1. *Suppose that* (H_1) *and* (H_2) *are respected for network (1) with* $\tau = 0,\ d_i \neq 0$ $(i = 1, 2, 3)$. *If at least one of* $(H_3) - (H_5)$ *is satisfied, then there exists* $k \in \mathrm{N}_0$ *such that network (1) will produce patterns induced by the Turing instability.*

Proof. Network (1) will be stable if all the Routh-Hurwitz criteria with respect to (7) $B_0(k^2) > 0,\ B_1(k^2) > 0,\ B_2(k^2) > 0$, and $B_0(k^2)B_1(k^2) > B_2(k^2)$ for $\forall\ k \in \mathrm{N}_0$. Violation of at least one of these previous stability conditions results in network (1) instability caused by diffusion. It is apparent that if (H_2) and any one of $(H_3) - (H_5)$ hold, then at least one of conditions of the Routh-Hurwitz criteria is not respected, i.e. $\forall\ \mathrm{Re}(\lambda_k) < 0$ for $k = 0$ and $\exists\ \mathrm{Re}(\lambda_k) > 0$ for $k \neq 0$. Thus, there exists $k \in \mathrm{N}_0$ such that network (1) will produce patterns induced by the Turing instability, which implies the proof is fulfilled. □

3.2. **The Hopf bifurcation analysis induced by delay.** In this section, we will study on the existence of the Hopf bifurcation of network (1). When $\tau = 0,\ d_i \neq 0$ $(i = 1e, 2, 3)$, the characteristic equation of network (5) is shown in (7). Let

$$J(k^2) = B_0(k^2)B_1(k^2) - B_2(k^2) = B_0^* k^6 + B_1^* k^4 + B_2^* k^2 + B_3^*,$$

in which

$$\begin{aligned} B_0^* &= B_{01}B_{11} - B_{21}, \\ B_1^* &= B_{01}B_{12} + \varphi_0 B_{11} - B_{22}, \\ B_2^* &= \varphi_1 B_{01} + \varphi_0 B_{12} - B_{23}, \\ B_3^* &= \varphi_0\varphi_1 - \varphi_2. \end{aligned}$$

We make the following hypotheses to define the stability of original network (1) with $\tau = 0,\ d_i \neq 0$ $(i = 1, 2, 3)$

$$\begin{aligned} &(H_6)\ B_{01} > 0,\ G(1) > 0; \\ &(H_7)\ B_{11} > 0,\ B_{12}^2 - 4B_{11}\varphi_1 < 0, \\ &\qquad \text{or } B_{11} > 0,\ B_{12} > 0,\ H(1) > 0; \\ &(H_8)\ B_{21} > 0,\ B_{23} < 0,\ I(x_+) > 0, \\ &\qquad \text{or } B_{21} > 0,\ B_{22} > 0,\ B_{23} > 0,\ I(1) > 0; \\ &(H_9)\ B_0^* > 0, B_1^* > 0, B_2^* > 0, B_3^* < 0, J(1) > 0. \end{aligned}$$

Lemma 5. *For* $G(k^2)$, $H(k^2)$, $I(k^2)$, $J(k^2)$, *we have the following results.*

1) If (H_6) *is satisfied, then* $G(k^2) > 0$ *for any positive integers* $k \in [1, +\infty)$.
2) If (H_7) *is satisfied, then* $H(k^2) > 0$ *for any positive integers* $k \in [1, +\infty)$.
3) If (H_8) *is satisfied, then* $I(k^2) > 0$ *for any positive integers* $k \in [1, +\infty)$.
4) If (H_9) *is satisfied, then* $J(k^2) > 0$ *for any positive integers* $k \in [1, +\infty)$.

Proof.

1) If $B_{01} > 0$ holds, we conclude that $G'(k^2) = B_{01} > 0$, which means that $G(k^2)$ is a monotonically increasing function of k^2. Owning to $G(1) > 0$, it is simple for us to find that $G(k^2) > 0$ for any positive natural numbers $k \in [1, +\infty)$. This completes the proof. The proof of the second assumption from (H_7) of 2), the second assumption from (H_8) of 3) and 4) are similar to that of 1), both adopt the monotonicity criterion to determine the sign of functions. Therefore, no further proof is given here.
2) Owning to $B_{11} > 0, B_{12}^2 - 4B_{11}\varphi_1 < 0, \varphi_1 < 0$, it is quite clear that $H(s) = B_{11}s^2 + B_{12}s + \varphi_1$ is a quadratic function that is always above the horizontal axis with the opening upwards. As a result, it is simple for us to derive that $H(k^2) > 0$ for any positive integers $k \in [1, +\infty)$. The proof of the first assumption from (H_7) of 2) is accomplished.

3) If $B_{21} > 0,\ B_{23} < 0,\ I(x_+) > 0$ are satisfied, $I(x)$ is always above the horizontal axis when $x \in (0, +\infty)$ that can be inferred from Lemma 4. Thus, we can speculate that $I(k^2) > 0$ for any positive integers $k \in [1, +\infty)$. The proof of the first assumption from (H_8) of 3) is accomplished. □

Theorem 2. *Suppose that* $(H_1),\ (H_6) - (H_9)$ *are respected for network (1) with* $\tau = 0,\ d_i \neq 0\ (i = 1, 2, 3)$.

1) The non-trivial equilibrium point $E^*(S^*, I^*, Y^*)$ *of network (1) is locally asymptotically stable at any positive integers* $k \in [1, +\infty)$.

2) The non-trivial equilibrium point $E^*(S^*, I^*, Y^*)$ *of network (1) is unstable.*

Proof. If $(H_6) - (H_9)$ are satisfied, it is not difficult to launch $B_0(k^2) > 0,\ B_1(k^2) > 0,\ B_2(k^2) > 0$, and $B_0(k^2)B_1(k^2) > B_2(k^2)$ for $\forall k \in \mathrm{N}$ and $B_0(0)B_1(0) < B_2(0)$ at $k = 0$. Accordingly, we infer that the non-trivial equilibrium point $E^*(S^*, I^*, Y^*)$ of network (1) is locally asymptotically stable except $k = 0$ through the Routh-Hurwitz criterion. □

Remark 5. *It is worth noting that* k *encompassing the location information of the reaction-diffusion network (1) is the eigenvalue of the Laplacian operator* Δ *on the region* $\Delta :\ \partial^2/\partial x^2$ *under the homogeneous the Neumann boundary condition. If the non-trivial equilibrium point* $E^*(S^*, I^*, Y^*)$ *of network (1) is to be locally asymptotically stable, it is required that* $\mathrm{Re}(\lambda_k) < 0$ *for* $\forall k \in \mathrm{N}_0$. *If there is one* $k \in \mathrm{N}_0$ *that is not satisfied, then the non-trivial equilibrium point* $E^*(S^*, I^*, Y^*)$ *of network (1) will become unstable.*

Assume that $\lambda = i\omega\ (\omega > 0)$ is a root of (5). Substituting $i\omega$ into (5) and separating the real and imaginary parts leads to

$$\begin{cases} (A_5(k^2) - A_3(k^2)\omega^2)\cos\omega\tau + A_4(k^2)\omega\sin\omega\tau = A_0(k^2)\omega^2 - A_2(k^2), \\ (A_5(k^2) - A_3(k^2)\omega^2)\sin\omega\tau - A_4(k^2)\omega\cos\omega\tau = A_1(k^2)\omega - \omega^3. \end{cases} \tag{8}$$

This yields

$$\omega^6 + C_0(k^2)\omega^4 + C_1(k^2)\omega^2 + C_2(k^2) = 0, \tag{9}$$

where

$$\begin{aligned} C_0(k^2) =& A_0^2(k^2) - 2A_1(k^2) - A_3^2(k^2) = (d_1k^2 - a_{11})^2 + (d_2k^2 - a_{22})^2 + (d_3k^2 - a_{33})^2 \\ & - b_{22}^2 + 2a_{12}a_{21} + 2a_{13}a_{31} + 2a_{23}a_{32}, \\ C_1(k^2) =& A_1^2(k^2) - 2A_0(k^2)A_2(k^2) + 2A_3(k^2)A_5(k^2) - A_4^2(k^2) \\ =& [2a_{11} + 2a_{22} + 2a_{33} - 2k^2(d_1 + d_2 + d_3)] \times [d_1d_2d_3k^6 - (a_{11}d_2d_3 + a_{22}d_1d_3 + a_{33}d_1d_2)k^4 \\ & + (a_{11}a_{22}d_3 - a_{12}a_{21}d_3 + a_{11}a_{33}d_2 - a_{13}a_{31}d_2 + a_{22}a_{33}d_1 - a_{23}a_{32}d_1)k^2 \\ & - a_{11}a_{22}a_{33} + a_{11}a_{23}a_{32} + a_{12}a_{21}a_{33} - a_{12}a_{23}a_{31} - a_{13}a_{21}a_{32} + a_{13}a_{22}a_{31}] \\ & - 2b_{22}[-b_{22}d_1d_3k^4 + (a_{11}b_{22}d_3 - a_{21}b_{12}d_3 + a_{33}b_{22}d_1)k^2 - a_{11}a_{33}b_{22} + a_{13}a_{31}b_{22} \\ & + a_{21}a_{33}b_{12} - a_{23}a_{31}b_{12}] + [(d_1d_2 + d_1d_3 + d_2d_3)k^4 - (a_{11}d_2 + a_{11}d_3 + a_{22}d_1 \\ & + a_{22}d_3 + a_{33}d_1 + a_{33}d_2)k^2 + a_{11}a_{22} - a_{12}a_{21} + a_{11}a_{33} - a_{13}a_{32} + a_{22}a_{33} - a_{23}a_{32}]^2 \\ & - [-(b_{22}d_1 + b_{22}d_3)k^2 + a_{11}b_{22} - a_{21}b_{12} + a_{33}b_{22}]^2, \end{aligned}$$

$$\begin{aligned} C_2(k^2) =& A_2^2(k^2) - A_5^2(k^2) = [-d_1d_2d_3k^6 + (a_{11}d_2d_3 + a_{22}d_1d_3 + a_{33}d_1d_2)k^4 \\ & + (a_{12}a_{21}d_3 - a_{11}a_{22}d_3 - a_{11}a_{33}d_2 + a_{13}a_{31}d_2 - a_{22}a_{33}d_1 + a_{23}a_{32}d_1)k^2 \\ & + a_{11}a_{22}a_{33} - a_{11}a_{23}a_{32} - a_{12}a_{21}a_{33} + a_{12}a_{23}a_{31} + a_{13}a_{21}a_{32} - a_{13}a_{22}a_{31}]^2 \\ & - [b_{22}d_1d_3k^4 + (a_{21}b_{12}d_3 - a_{11}b_{22}d_3 - a_{33}b_{22}d_1)k^2 + a_{11}a_{33}b_{22} - a_{21}a_{33}b_{12} \\ & - a_{13}a_{32}b_{22} + a_{23}a_{32}b_{12}]^2. \end{aligned}$$

Define $z = \omega^2$, then (9) is reduced into

$$z^3 + C_0(k^2)z^2 + C_1(k^2)z + C_2(k^2) = 0. \tag{10}$$

When $k = 0$, if the following hypothesis holds

$$\begin{aligned}(H_{10})\ C_2(0) =&(a_{11}a_{22}a_{33} - a_{11}a_{23}a_{32} - a_{12}a_{21}a_{33} + a_{12}a_{23}a_{31} + a_{13}a_{21}a_{32} - a_{13}a_{22}a_{31})^2\\ &- (a_{11}a_{33}b_{22} - a_{13}a_{31}b_{22} - a_{21}a_{33}b_{12} + a_{23}a_{31}b_{12})^2 < 0,\end{aligned}$$

then (10) has at least one root with a positive real part at $k = 0$. Without loss of generality, we may wish to suppose that (10) has three positive real roots $z_i > 0$ $(i = 1, 2, 3)$, so that the characteristic equation (5) possesses three pair of purely imaginary roots $\pm i\omega_i$ $(\omega_i = \sqrt{z_i},\ i = 1, 2, 3)$ when $\tau = \tau_{i,0}^{(j)},\ j = 0, 1, 2\ldots$, which is calculated by (8)

$$\tau_{i,0}^{(j)} =$$

$$\frac{1}{\omega_i}\left\{\arccos\left[\frac{(A_0(0)\omega_i^2 - A_2(0))(A_5(0) - A_3(0)\omega_i^2) - (A_1(0)\omega_i - \omega_i^3)A_4(0)\omega_i}{(A_5(0) - A_3(0)\omega_i^2)^2 + A_4^2(0)\omega_i^2}\right] + 2j\pi\right\}. \tag{11}$$

When $k \geq 1$, let $\vartheta = k^2$, then define

$$\zeta(\vartheta) = C_0(\vartheta),\ \xi(\vartheta) = C_1(\vartheta),\ \Xi(\vartheta) = C_2(\vartheta).$$

We establish the following hypothesis

$$\begin{aligned}(H_{11})\ &\zeta(1) > 0,\ \xi(1) > 0,\ \Xi(1) > 0,\\ &\zeta'(\vartheta) > 0,\ \xi'(\vartheta) > 0,\ \Xi'(\vartheta) > 0 \text{ for } \forall\vartheta \geq 1.\end{aligned}$$

If (H_{11}) holds, it is obvious that (10) has no roots with positive real part when $k \geq 1$. Then we define that

$$\tau_0 = \tau_{i_0,0}^{(0)} = \min_{i=\{1,2,3\}}\left\{\tau_{i,0}^{(0)}\right\}, \omega_0 = \omega_{i_0}. \tag{12}$$

Substituting $\lambda(\tau)$ into (5) when $k = 0$, and taking the derivative of both sides of (5) with respect to τ gives

$$\left[\frac{d\lambda}{d\tau}\right]^{-1} = \frac{Q_1(\lambda)}{Q_2(\lambda)} - \frac{\tau}{\lambda},$$

in which

$$\begin{aligned}Q_1(\lambda) &= 3\lambda^2 + 2A_0(0)\lambda + A_1(0) + e^{-\lambda\tau}[2A_3(0)\lambda + A_4(0)],\\ Q_2(\lambda) &= \lambda e^{-\lambda\tau}(A_3(0)\lambda^2 + A_4(0)\lambda + A_5(0)).\end{aligned}$$

Assume that $\lambda(\tau) = \delta(\tau) + i\varepsilon(\tau)$ is the root of (5) satisfying $\delta(\tau_0) = 0, \varepsilon(\tau_0) = \omega_0$, then we obtain that

$$\mathrm{Re}\left(\frac{d\lambda}{d\tau}\right)^{-1}_{\substack{\omega=\omega_0\\ \tau=\tau_0}} = \frac{M_1N_1 + M_2N_2}{N_1^2 + N_2^2},$$

where

$$\begin{aligned}M_1 &= -3\omega_0^2 + A_1(0) + A_4(0)\cos\omega_0\tau_0 + 2A_3(0)\omega_0\sin\omega_0\tau_0,\\ M_2 &= 2A_0(0)\omega_0 + 2A_3(0)\omega_0\cos\omega_0\tau_0 - A_4(0)\sin\omega_0\tau_0,\\ N_1 &= -A_4(0)\omega_0^2\cos\omega_0\tau_0 + (-A_3(0)\omega_0^2 + A_5(0))\omega_0\sin\omega_0\tau_0,\\ N_2 &= (-A_3(0)\omega_0^2 + A_5(0))\omega_0\cos\omega_0\tau_0 + A_4(0)\omega_0^2\sin\omega_0\tau_0.\end{aligned}$$

If following hypothesis (H_{12}) holds

$$(H_{12})\ M_1N_1 + M_2N_2 \neq 0,$$

then the transversality condition of network (1) when $\tau = \tau_0$.

Theorem 3. *Suppose that* (H_1), $(H_6)-(H_{12})$ *are respected for network (1) with* $\tau \neq 0$, $d_i \neq 0$ $(i=1,2,3)$.

1) *When* $\tau \in [0,\tau_0)$, *then the non-trivial equilibrium point* $E^*(S^*,I^*,Y^*)$ *of network (1) is unstable.*
2) *When* $\tau > \tau_0$, *then the non-trivial equilibrium point* $E^*(S^*,I^*,Y^*)$ *of network (1) is locally asymptotically stable and a family of spatiotemporal periodic solutions converge to the non-trivial equilibrium point* $E^*(S^*,I^*,Y^*)$ *at* $\tau=\tau_0$.

4. Direction and stability of the Hopf bifurcation

In this section, we will calculate the normal form of the Hopf bifurcation on the center manifold. To investigate the dynamical behaviors of network (1) in the vicinity of the Hopf bifurcation point, we will study the normal form of the Hopf bifurcation through making use of the normal form method of partial functional differential equations.

Let $u(x,t)=S(x,\tau t), v(x,t)=I(x,\tau t), w(x,t)=Y(x,\tau t)$. For the sake of representation, denote $U(t)=U(\cdot,t)=(u(\cdot,t),v(\cdot,t),w(\cdot,t))^T$ and $U_t(\theta)=U(t+\theta)=(U_{1t}(\theta),U_{2t}(\theta),U_{3t}(\theta))^T$. Then, network (2) is transformed into a functional differential equation in $C([-1,0],\mathbb{R}^3)$ as

$$\frac{\partial U(t)}{\partial t}=D_\mu \Delta U(t)+L_\mu(U_t)+F(\mu,U_t), \tag{13}$$

where

$$\begin{aligned}
&D_\mu=(\tau_0+\mu)D,\\
&L_\mu(U_t)=(\tau_0+\mu)(MU_t(0)+NU_t(-1)),\\
&F(\mu,U_t)=(\tau_0+\mu)\begin{pmatrix} F_1+h.o.t.\\ F_2+h.o.t.\\ F_3+h.o.t.\end{pmatrix},
\end{aligned}$$

and

$$\begin{aligned}
F_1=&a_{14}U_{1t}^2(0)+a_{15}U_{1t}(0)U_{2t}(0)+a_{16}U_{1t}(0)U_{3t}(0)+b_{13}U_{1t}(0)U_{2t}(-1)+b_{14}U_{2t}^2(-1)\\
&+b_{15}U_{1t}(0)U_{2t}^2(-1)+b_{16}U_{2t}^3(-1),\\
F_2=&a_{24}U_{2t}(0)U_{3t}(0)+b_{23}U_{1t}(0)U_{2t}(-1)+b_{24}U_{2t}^2(-1)+b_{25}U_{1t}(0)U_{2t}^2(-1)+b_{26}U_{2t}^3(-1),\\
F_3=&a_{34}U_{1t}(0)U_{3t}(0)+a_{35}U_{2t}(0)U_{3t}(0).
\end{aligned}$$

In the previous section, we have obtained that network (1) is unstable and a family of periodic spatiotemporal solutions appear at $\tau=\tau_0$. We introduce parameter μ by setting $\tau=\tau_0+\mu$, and $\mu=0$ is the Hopf bifurcation value of network (1). $\Lambda_0=\{\pm i\omega_0\tau_0\}$ are a pair of purely imaginary characteristic roots of the following linearized representation of (13) with $\mu=0$

$$\frac{\partial U(t)}{\partial t}=D_0\Delta U(t)+L_0(U_t). \tag{14}$$

Define

$$\frac{\partial z(t)}{\partial t}=L_0(z_t).$$

Obviously, L_0 is a continuous linear operator vector mapping $\mathcal{C}:=\mathcal{C}([-1,0],\mathbb{R}^3)$. Through the Riesz representation theorem, there exists a 3×3 matrix function $\eta_k(\mu,\theta),\theta\in[-1,0]$ whose entries are of bounded variation such that

$$-k^2D_\mu U(t)+L_\mu(U_t)=\int_{-1}^{0} d\eta_k(\mu,\theta)U_t(\theta),\phi\in\mathcal{C}.$$

In fact, we can choose

$$\eta_k(\mu,\theta)=\begin{cases}0,\ \theta=-1,\\ (\tau_0+\mu)N,\ \theta\in(-1,0),\\ (\tau_0+\mu)(M+N),\ \theta=0.\end{cases} \tag{15}$$

For the sake of simplification, we write $\eta_k(\theta)$ instead of $\eta_k(0,\theta)$. Denote $\mathfrak{A}$ as the infinitesimal generator of the semigroup generated by (14) with $\mu=0$ and $k=0$ and, the adjoint operator $\mathfrak{A}^*$ of $\mathfrak{A}$ on $\mathcal{C}^*:=\mathcal{C}([0,1],(\mathbb{R}^3)^*)$ as

$$\mathfrak{A}^*\psi(s)=\begin{cases}-\dot{\psi}(s),\ s\in(0,1],\\ \int\limits_{-1}^{0}\psi(-\theta)d\eta_0(\theta),\ s=0,\end{cases}$$

with the bilinear form

$$\langle\psi,\varphi\rangle=\bar{\psi}(0)\varphi(0)-\int\limits_{\theta=-1}^{0}\int\limits_{\xi=0}^{\theta}\overline{\psi}(\xi-\theta)d\eta_0(\theta)\varphi(\xi)d\xi. \tag{16}$$

Let $q(\theta)=q(0)e^{i\omega_0\tau_0\theta}$ $(\theta\in[-1,0])$, $q^*(s)=q^*(0)e^{i\omega_0\tau_0 s}$ $(s\in[0,1])$ be the feature vectors of $\mathfrak{A}$ and $\mathfrak{A}^*$ corresponding to $i\omega_0\tau$ and $-i\omega_0\tau$, respectively. Suppose that $q(\theta)=(1,\iota,\kappa)^Te^{i\omega_0\tau_0\theta}$ is the feature vector of $\mathfrak{A}$. Then, $Aq(\theta)=i\omega_0\tau_0q(\theta)$. It follows from the definition of $\mathfrak{A}$ and (15) that

$$\tau_0\begin{bmatrix}i\omega_0-a_{11} & -a_{12}-b_{12}e^{-i\omega_0\tau_0} & -a_{13}\\ -a_{21} & i\omega_0-a_{22}-b_{22}e^{-i\omega_0\tau_0} & -a_{23}\\ -a_{31} & -a_{32} & i\omega_0-a_{33}\end{bmatrix}q(0)=\begin{bmatrix}0\\0\\0\end{bmatrix},$$

which yields

$$\iota=\frac{(i\omega_0-a_{33})a_{21}+a_{23}a_{31}}{(i\omega_0-a_{22}-b_{22}e^{-i\omega_0\tau_0})(i\omega_0-a_{33})-a_{23}a_{32}},$$
$$\kappa=\frac{(i\omega_0-a_{22}-b_{22}e^{-i\omega_0\tau_0})a_{31}+a_{21}a_{32}}{(i\omega_0-a_{22}-b_{22}e^{-i\omega_0\tau_0})(i\omega_0-a_{33})-a_{23}a_{32}}.$$

Similarity, it can be verified that $q^*(s)=D(1,\iota^*,\kappa^*)e^{i\omega_0\tau_0 s}$ is the feature vector of $\mathfrak{A}^*$ corresponding to $-i\omega_0\tau_0$, where

$$\iota^*=\frac{-(i\omega_0+a_{11})(i\omega_0+a_{33})+a_{13}a_{31}}{a_{21}(i\omega_0+a_{33})-a_{23}a_{31}},$$
$$\kappa^*=\frac{(i\omega_0+a_{11})a_{23}-a_{13}a_{21}}{a_{21}(i\omega_0+a_{33})-a_{23}a_{31}}.$$

By means of (16), we obtain

$$\begin{aligned}\langle q^*(s),q(\theta)\rangle=&\bar{D}(1,\overline{\iota^*},\overline{\kappa^*})(1,\iota,\kappa)^T-\int\limits_{\theta=-1}^{0}\int\limits_{\xi=0}^{\theta}\bar{D}(1,\overline{\iota^*},\overline{\kappa^*})e^{-i\omega_0\tau_0(\xi-\theta)}d\eta_0(\theta)(1,\iota,\kappa)^Te^{i\omega_0\tau_0\xi}\\ =&\bar{D}\left\{1+\iota\overline{\iota^*}+\kappa\overline{\kappa^*}-\int\limits_{\theta=-1}^{0}(1,\overline{\iota^*},\overline{\kappa^*})\theta e^{i\omega_0\tau_0\theta}d\eta_0(\theta)(1,\iota,\kappa)^T\right\}\\ =&\bar{D}\{1+\iota\overline{\iota^*}+\kappa\overline{\kappa^*}+(1,\overline{\iota^*},\overline{\kappa^*})\tau_0Ne^{-i\omega_0\tau_0}(1,\iota,\kappa)^T\}.\end{aligned}$$

Therefore, we can choose

$$D=\frac{1}{1+\bar{\iota}\iota^*+\bar{\kappa}\kappa^*+\tau_0e^{i\omega_0\tau_0}\bar{\iota}(b_{12}+b_{22}\iota^*)},$$

such that $\langle q^*(s), q(\theta)\rangle = 1$.

In the following, utilizing the same notations in [15], we compute the coordinates to describe the center manifold $\mathcal{C}_0$ at $\mu = 0$ and $k = 0$. We know U_t is the solution of (13), and denote

$$\mathfrak{z}(t) = \langle q^*, U_t\rangle\,,\ W(t,\theta) = U_t(\theta) - \mathfrak{z}(t)q(\theta) - \bar{\mathfrak{z}}(t)\bar{q}(\theta) = U_t(\theta) - 2\mathrm{Re}\{\mathfrak{z}(t)q(\theta)\}.$$

On the center mainfold $\mathcal{C}_0$, we have

$$W(t,\theta) = (\mathfrak{z}(t), \bar{\mathfrak{z}}(t), \theta)\,,$$

where

$$W(\mathfrak{z},\bar{\mathfrak{z}},\theta) = W_{20}(\theta)\frac{\mathfrak{z}^2}{2} + W_{11}(\theta)\mathfrak{z}\bar{\mathfrak{z}} + W_{02}(\theta)\frac{\bar{\mathfrak{z}}^2}{2} + W_{30}(\theta)\frac{\mathfrak{z}^3}{6} + \cdots,$$

$\mathfrak{z}$ and $\bar{\mathfrak{z}}$ are local coordinates for center manifold $\mathcal{C}_0$ in the direction of q^* and $\overline{q^*}$, respectively. Notice that W is real if U_t is real. We consider only real solutions. For the solution $U_t \in \mathcal{C}_0$ of (13), since $\mu = 0$ and $k = 0$, we have

$$\begin{aligned}\dot{\mathfrak{z}} &= i\omega_0\tau_0\mathfrak{z} + \langle q^*(\theta), F(0, W(\mathfrak{z},\bar{\mathfrak{z}},0) + 2\mathrm{Re}\{\mathfrak{z}q(\theta)\})\rangle\\ &= i\omega_0\tau_0\mathfrak{z} + \overline{q^*}(0)F(0, W(\mathfrak{z},\bar{\mathfrak{z}},0) + 2\mathrm{Re}\{\mathfrak{z}q(0)\})\\ &\overset{def}{=} i\omega_0\tau_0\mathfrak{z} + \overline{q^*}(0)F_0(\mathfrak{z},\bar{\mathfrak{z}}).\end{aligned}$$

It can be denoted as

$$\dot{\mathfrak{z}}(t) = i\omega_0\tau_0\mathfrak{z}(t) + g(\mathfrak{z},\bar{\mathfrak{z}}),$$

with

$$g(\mathfrak{z},\bar{\mathfrak{z}}) = \overline{q^*}(0)F_0(\mathfrak{z},\bar{\mathfrak{z}}) = g_{20}\frac{\mathfrak{z}^2}{2} + g_{11}\mathfrak{z}\bar{\mathfrak{z}} + g_{02}\frac{\bar{\mathfrak{z}}^2}{2} + g_{21}\frac{\mathfrak{z}^2\bar{\mathfrak{z}}}{2} + \cdots. \tag{17}$$

In the preceding statement, we have $U_t(\theta) = U(t+\theta) = (U_{1t}(\theta), U_{2t}(\theta), U_{3t}(\theta))^T = W(t,\theta) + zq(\theta) + \bar{z}\bar{q}(\theta)$ and $q(\theta) = (1,\iota,\kappa)^T e^{i\omega_0\tau_0\theta}$, and then

$$\begin{aligned}&\overline{q^*}(0) = \bar{D}(1,\overline{\iota^*},\overline{\kappa^*}),\\ &U_{1t}(0) = \mathfrak{z} + \bar{\mathfrak{z}} + W_{20}^{(1)}(0)\frac{\mathfrak{z}^2}{2} + W_{11}^{(1)}(0)\mathfrak{z}\bar{\mathfrak{z}} + W_{02}^{(1)}(0)\frac{\bar{\mathfrak{z}}^2}{2} + O(|(\mathfrak{z},\bar{\mathfrak{z}})^3|),\\ &U_{2t}(0) = \mathfrak{z}\iota + \bar{\mathfrak{z}}\bar{\iota} + W_{20}^{(2)}(0)\frac{\mathfrak{z}^2}{2} + W_{11}^{(2)}(0)\mathfrak{z}\bar{\mathfrak{z}} + W_{02}^{(2)}(0)\frac{\bar{\mathfrak{z}}^2}{2} + O(|(\mathfrak{z},\bar{\mathfrak{z}})^3|),\\ &U_{2t}(-1) = \mathfrak{z}\iota e^{-i\omega_0\tau_0} + \bar{\mathfrak{z}}\bar{\iota}e^{i\omega_0\tau_0} + W_{20}^{(2)}(-1)\frac{\mathfrak{z}^2}{2} + W_{11}^{(2)}(-1)\mathfrak{z}\bar{\mathfrak{z}} + W_{02}^{(2)}(-1)\frac{\bar{\mathfrak{z}}^2}{2} + O(|(\mathfrak{z},\bar{\mathfrak{z}})^3|),\\ &U_{3t}(0) = \mathfrak{z}\kappa + \bar{\mathfrak{z}}\bar{\kappa} + + W_{20}^{(3)}(0)\frac{\mathfrak{z}^2}{2} + W_{11}^{(3)}(0)\mathfrak{z}\bar{\mathfrak{z}} + W_{02}^{(3)}(0)\frac{\bar{\mathfrak{z}}^2}{2} + O(|(\mathfrak{z},\bar{\mathfrak{z}})^3|).\end{aligned}$$

It follows together with (13) that

$$\begin{aligned}&g(\mathfrak{z},\bar{\mathfrak{z}}) = \overline{q^*}(0)F_0(z,\bar{z})\\ =&\bar{D}\tau_0(1,\overline{\iota^*},\overline{\kappa^*})\begin{pmatrix} a_{14}U_{1t}^2(0) + a_{15}U_{1t}(0)U_{2t}(0) + a_{16}U_{1t}(0)U_{3t}(0) + b_{13}U_{1t}(0)U_{2t}(-1)\\ +b_{14}U_{2t}^2(-1) + b_{15}U_{1t}(0)U_{2t}^2(-1) + b_{16}U_{2t}^3(-1),\\ a_{24}U_{2t}(0)U_{3t}(0) + b_{23}U_{1t}(0)U_{2t}(-1) + b_{24}U_{2t}^2(-1) + b_{25}U_{1t}(0)U_{2t}^2(-1)\\ +b_{26}U_{2t}^3(-1),\\ a_{34}U_{1t}(0)U_{3t}(0) + a_{35}U_{2t}(0)U_{3t}(0),\end{pmatrix}.\end{aligned}$$

Comparing the coefficients with (17), we have

$$
\begin{aligned}
g_{20} =&2\bar{D}\tau_0[a_{14}+a_{15}\iota+a_{16}\kappa+b_{13}\iota e^{-i\omega_0\tau_0}+b_{14}\iota^2e^{-2i\omega_0\tau_0}\\
&+\overline{\iota^*}(a_{24}\kappa\iota+b_{23}\iota e^{-i\omega_0\tau_0}+b_{24}\iota^2e^{-2i\omega_0\tau_0})\\
&+\overline{\kappa^*}(a_{34}\kappa+a_{35}\iota\kappa)],\\
g_{11} =&\bar{D}\tau_0[2a_{14}+a_{15}\bar{\iota}+a_{15}\iota+a_{16}\bar{\kappa}+a_{16}\kappa+b_{13}\bar{\iota}e^{i\omega_0\tau_0}+b_{13}\iota e^{-i\omega_0\tau_0}+2b_{14}\iota\bar{\iota}\\
&+\overline{\iota^*}(a_{24}\bar{\kappa}\iota+a_{24}\kappa\bar{\iota}+b_{23}\bar{\iota}e^{i\omega_0\tau_0}+b_{23}\iota e^{-i\omega_0\tau_0}+2b_{24}\iota\bar{\iota})\\
&+\overline{\kappa^*}(a_{34}\bar{\kappa}+a_{34}\kappa+a_{35}\iota\bar{\kappa}+a_{35}\bar{\iota}\kappa)],\\
g_{02} =&2\bar{D}\tau_0[a_{14}+a_{15}\bar{\iota}+a_{16}\bar{\kappa}+b_{13}\bar{\iota}e^{i\omega_0\tau_0}+b_{14}\bar{\iota}^2e^{2i\omega_0\tau_0}\\
&+\overline{\iota^*}(a_{24}\bar{\kappa}\bar{\iota}+b_{23}\bar{\iota}e^{i\omega_0\tau_0}+b_{24}\bar{\iota}^2e^{2i\omega_0\tau_0})+\kappa^*(a_{34}\bar{\kappa}+a_{35}\bar{\iota}\bar{\kappa})],\\
g_{21} =&2\bar{D}\tau_0[a_{14}(2W_{11}^{(1)}(0)+W_{20}^{(1)}(0))+a_{15}(W_{11}^{(2)}(0)+\frac{1}{2}W_{20}^{(2)}(0)+\frac{1}{2}W_{20}^{(1)}(0)\bar{\iota}+W_{11}^{(1)}(0)\iota)\\
&+a_{16}(W_{11}^{(3)}(0)+\frac{1}{2}W_{20}^{(3)}(0)+\frac{1}{2}W_{20}^{(1)}(0)\bar{\kappa}+W_{11}^{(1)}(0)\kappa)\\
&+b_{13}(W_{11}^{(2)}(-1)+\frac{1}{2}W_{20}^{(2)}(-1)+\frac{1}{2}W_{20}^{(1)}(0)\bar{\iota}e^{i\omega_0\tau_0}+W_{11}^{(1)}(0)\iota e^{-i\omega_0\tau_0})\\
&+b_{14}(2\iota W_{11}^{(2)}(-1)+\bar{\iota}W_{20}^{(2)}(-1))+b_{15}(2\iota\bar{\iota}+\iota^2e^{-2i\omega_0\tau_0})+3b_{16}\iota^2\bar{\iota}e^{-i\omega_0\tau_0}\\
&+\overline{\iota^*}a_{24}(W_{11}^{(3)}(0)\iota+\frac{1}{2}W_{20}^{(3)}(0)\bar{\iota}+\frac{1}{2}W_{20}^{(2)}(0)\bar{\kappa}+W_{11}^{(2)}(0)\kappa)\\
&+\overline{\iota^*}b_{23}(W_{11}^{(2)}(-1)+\frac{1}{2}W_{20}^{(2)}(-1)+\frac{1}{2}W_{20}^{(1)}(0)\bar{\iota}e^{i\omega_0\tau_0}+W_{11}^{(1)}(0)\iota e^{-i\omega_0\tau_0})\\
&+\overline{\iota^*}b_{24}(2\iota W_{11}^{(2)}(-1)+\bar{\iota}W_{20}^{(2)}(-1))+\overline{\iota^*}b_{25}(2\iota\bar{\iota}+\iota^2e^{-2i\omega_0\tau_0})\\
&+\overline{\kappa^*}a_{34}(W_{11}^{(3)}(0)+\frac{1}{2}W_{20}^{(3)}(0)+\frac{1}{2}W_{20}^{(1)}(0)\bar{\kappa}+W_{11}^{(1)}(0)\kappa)\\
&+\overline{\kappa^*}a_{35}(W_{11}^{(3)}(0)\iota+\frac{1}{2}W_{20}^{(3)}(0)\bar{\iota}+\frac{1}{2}W_{20}^{(2)}(0)\bar{\kappa}+W_{11}^{(2)}(0)\kappa)].
\end{aligned}
$$

with

$$W_{20}(\theta)=\frac{ig_{20}}{\omega_0\tau_0}q(0)e^{i\omega_0\tau_0\theta}-\frac{i\bar{g}_{02}}{3\omega_0\tau_0}\bar{q}(0)e^{-i\omega_0\tau_0\theta}+E_1e^{2i\omega_0\tau_0\theta},$$

and

$$W_{11}(\theta)=-\frac{ig_{11}}{\omega_0\tau_0}q(0)e^{i\omega_0\tau_0\theta}+\frac{i\bar{g}_{11}}{\omega_0\tau_0}\bar{q}(0)e^{-i\omega_0\tau_0\theta}+E_2.$$

The expressions of $E_1=(E_1^{(1)},E_1^{(2)},E_1^{(3)})^T$ and $E_2=(E_2^{(1)},E_2^{(2)},E_2^{(3)})^T$ are as follows:

$$
\begin{aligned}
E_1^{(1)} =&\frac{2}{\Upsilon}\begin{vmatrix} a_{14}+a_{15}\iota+a_{16}\kappa+b_{13}\iota e^{-i\omega_0\tau_0}+b_{14}\iota^2e^{-2i\omega_0\tau_0} & -a_{12}-b_{12}e^{-2i\omega_0\tau_0} & -a_{13}\\ a_{24}\kappa\iota+b_{23}\iota e^{-i\omega_0\tau_0}+b_{24}\iota^2e^{-2i\omega_0\tau_0} & 2i\omega_0-a_{22}-b_{22}e^{-2i\omega_0\tau_0} & -a_{23}\\ a_{34}\kappa+a_{35}\iota\kappa & -a_{32} & 2i\omega_0-a_{33}\end{vmatrix},\\
E_1^{(2)} =&\frac{2}{\Upsilon}\begin{vmatrix} 2i\omega_0-a_{11} & a_{14}+a_{15}\iota+a_{16}\kappa+b_{13}\iota e^{-i\omega_0\tau_0}+b_{14}\iota^2e^{-2i\omega_0\tau_0} & -a_{13}\\ -a_{21} & a_{24}\kappa\iota+b_{23}\iota e^{-i\omega_0\tau_0}+b_{24}\iota^2e^{-2i\omega_0\tau_0} & -a_{23}\\ -a_{31} & a_{34}\kappa+a_{35}\iota\kappa & 2i\omega_0-a_{33}\end{vmatrix},\\
E_1^{(3)} =&\frac{2}{\Upsilon}\begin{vmatrix} 2i\omega_0-a_{11} & -a_{12}-b_{12}e^{-2i\omega_0\tau_0} & a_{14}+a_{15}\iota+a_{16}\kappa+b_{13}\iota e^{-i\omega_0\tau_0}+b_{14}\iota^2e^{-2i\omega_0\tau_0}\\ -a_{21} & 2i\omega_0-a_{22}-b_{22}e^{-2i\omega_0\tau_0} & a_{24}\kappa\iota+b_{23}\iota e^{-i\omega_0\tau_0}+b_{24}\iota^2e^{-2i\omega_0\tau_0}\\ -a_{31} & -a_{32} & a_{34}\kappa+a_{35}\iota\kappa\end{vmatrix},
\end{aligned}
$$

in which

$$\Upsilon = \begin{vmatrix} 2i\omega_0 - a_{11} & -a_{12} - b_{12}e^{-2i\omega_0\tau_0} & -a_{13} \\ -a_{21} & 2i\omega_0 - a_{22} - b_{22}e^{-2i\omega_0\tau_0} & -a_{23} \\ -a_{31} & -a_{32} & 2i\omega_0 - a_{33} \end{vmatrix},$$

and

$$E_2^{(1)} = \frac{1}{\Xi}\begin{vmatrix} 2a_{14} + a_{15}\bar{\iota} + a_{15}\iota + a_{16}\bar{\kappa} + a_{16}\kappa + b_{13}\bar{\iota}e^{i\omega_0\tau_0} + \iota e^{-i\omega_0\tau_0} + 2b_{14}\iota\bar{\iota} & -a_{12} - b_{12} & -a_{13} \\ a_{24}\bar{\kappa}\iota + a_{24}\kappa\bar{\iota} + b_{23}\bar{\iota}e^{i\omega_0\tau_0} + b_{23}\iota e^{-i\omega_0\tau_0} + 2b_{24}\iota\bar{\iota} & -a_{22} - b_{22} & -a_{23} \\ a_{34}\bar{\kappa} + a_{34}\kappa + a_{35}\iota\bar{\kappa} + a_{35}\bar{\iota}\kappa & -a_{32} & -a_{33} \end{vmatrix},$$

$$E_2^{(2)} = \frac{1}{\Xi}\begin{vmatrix} -a_{11} & 2a_{14} + a_{15}\bar{\iota} + a_{15}\iota + a_{16}\bar{\kappa} + a_{16}\kappa + b_{13}\bar{\iota}e^{i\omega_0\tau_0} + \iota e^{-i\omega_0\tau_0} + 2b_{14}\iota\bar{\iota} & -a_{13} \\ -a_{21} & a_{24}\bar{\kappa}\iota + a_{24}\kappa\bar{\iota} + b_{23}\bar{\iota}e^{i\omega_0\tau_0} + b_{23}\iota e^{-i\omega_0\tau_0} + 2b_{24}\iota\bar{\iota} & -a_{23} \\ -a_{31} & a_{34}\bar{\kappa} + a_{34}\kappa + a_{35}\iota\bar{\kappa} + a_{35}\bar{\iota}\kappa & -a_{33} \end{vmatrix},$$

$$E_2^{(3)} = \frac{1}{\Xi}\begin{vmatrix} -a_{11} & -a_{12} - b_{12} & 2a_{14} + a_{15}\bar{\iota} + a_{15}\iota + a_{16}\bar{\kappa} + a_{16}\kappa + b_{13}\bar{\iota}e^{i\omega_0\tau_0} + \iota e^{-i\omega_0\tau_0} + 2b_{14}\iota\bar{\iota} \\ -a_{21} & -a_{22} - b_{22} & a_{24}\bar{\kappa}\iota + a_{24}\kappa\bar{\iota} + b_{23}\bar{\iota}e^{i\omega_0\tau_0} + b_{23}\iota e^{-i\omega_0\tau_0} + 2b_{24}\iota\bar{\iota} \\ -a_{31} & -a_{32} & a_{34}\bar{\kappa} + a_{34}\kappa + a_{35}\iota\bar{\kappa} + a_{35}\bar{\iota}\kappa \end{vmatrix},$$

in which

$$\Xi = \begin{vmatrix} -a_{11} & -a_{12} - b_{12} & -a_{13} \\ -a_{21} & -a_{22} - b_{22} & -a_{23} \\ -a_{31} & -a_{32} & -a_{33} \end{vmatrix}.$$

Then, g_{21} can be confirmed. Therefore, we can calculate the following quantities:

$$\begin{aligned} c_1(0) &= \frac{i}{2\omega_0\tau_0}(g_{20}g_{11} - 2|g_{11}|^2 - \frac{1}{3}|g_{02}|^2) + \frac{1}{2}g_{21}, \\ \mu_2 &= -\frac{\mathrm{Re}(c_1(0))}{\mathrm{Re}\lambda'(\tau_0)}, \\ \beta_2 &= 2\mathrm{Re}(c_1(0)), \\ T_2 &= -\frac{1}{\omega_0\tau_0}(\mathrm{Im}(c_1(0))) + \mu_2\mathrm{Im}(\lambda'(\tau_0))), \end{aligned} \tag{18}$$

where the sign of μ_2 determines the direction of the Hopf bifurcation, the sign of β_2 determines the stability of the bifurcating periodic solutions, and the sign of T_2 determines the period of the bifurcating periodic solutions. According to the analysis above, we have the following.

Theorem 4. *For network (1), if $\mu_2 > 0$ ($\mu_2 < 0$), the Hopf bifurcation is supercritical (subcritical). If $\beta_2 < 0$ ($\beta_2 > 0$), the bifurcating periodic solutions are stable (unstable). If $T_2 > 0$ ($T_2 < 0$), the period of the bifurcating periodic solutions increases (decreases).*

5. Numerical simulations

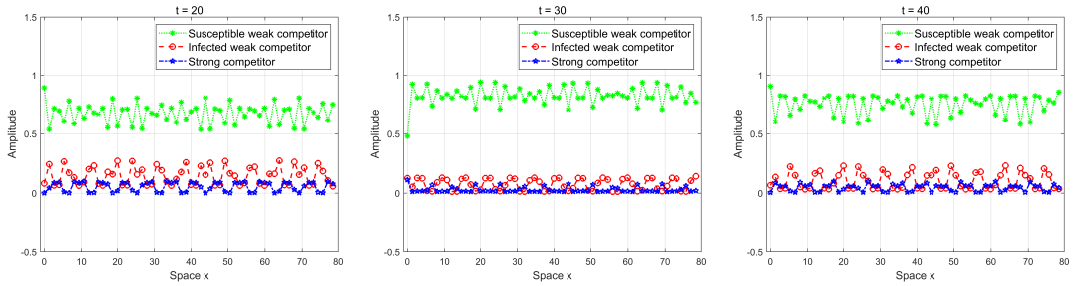
In this section, we analyze and illustrate the spatiotemporal dynamic mutations (the formation of stationary patterns induced by the Turing instability and the occurrence and extinction of spatial-temporal oscillations induced by the Hopf bifurcation) of network (1) in one dimensional space. Adopted the forward Euler finite difference method which utilizes the central difference quotient for the spatial scale and the forward difference quotient for the temporal scale [13], the stationary distribution (patterns) effected by diffusivity d and spatial-temporal solutions effected by incubation period τ are protracted in the following subsections, respectively. Last but not least, the properties of the Hopf bifurcation are further deduced with the aim of the normal form method and centre mainfold theorem.

5.1. **Impact of diffusivity d on the Turing instability.** In this subsection, we diagram the formation and evolution of different kinds of one-dimensional patterns due to the Turing instability induced by the variation of diffusivity d_2. Network (1) is studied on on a rectangular region where horizontal direction represents spatial scale $\Omega = (0, 25\pi)$ and the vertical direction represents temporal scale $t = (0, 100)$ under the homogeneous the Neumann boundary conditions and the initial conditions are $(0.01 + S^* + 0.01cos(x),\ 0.01 + I^* + 0.01cos(x),\ 0.01 + Y^* + 0.01cos(x))$. It is well known that the network dynamics depends on the choice of the initial conditions. If the initial spatial distribution of competitors is homogeneous, then the competitors distribution remains homogeneous forever. Significantly, the final instant at which we stopped the simulations is sufficient to suppose that the patterns arrive at the stationary state and they do not change and evolve further over time. For the subsequent simulations of the network, the initial conditions have been taken as a uniformly distributed random perturbation around the non-trivial equilibrium point $E^*(S^*, I^*, Y^*)$. For the choice of the parameter values in our network (1) are taken from [31], please see Table 2.

Table 2. Numerical values of parameters of network (1) taken from [31].

Parameters	Numerical values
The environment carrying capacity for weak competitor (K)	1
The intrinsic growth rate of susceptible weak competitor (a)	0.6
The natural death rate of infected weak competitor (c)	0.25
The natural death rate of strong competitor (d)	0.5
The prevention coefficient of epidemic (α)	0.5
The infection coefficient of epidemic (β)	0.7
The coefficient of predation for susceptible weak competitor to strong competitor (p_1)	0.125
The coefficient of predation for infected weak competitor to strong competitor (p_2)	6
The coefficient of conversing weak competitor to strong competitor (q)	0.75
The incubation period delay of the epidemic in weak competitor (τ)	0

We fix the susceptible weak competitor diffusivity $d_1 = -0.01$ and strong competitor diffusivity $d_3 = 0.01$, where d_1 is selected as anomalous negative self-diffusion coefficient, signifying the transfer of the susceptible weak competitor from low-density regions to high-density regions. We examine the patterns evolution behaviors near the homogeneous non-trivial equilibrium point $E^*(0.7903,\ 0.0946,\ 0.0464)$ at different infected weak competitor diffusivity $d_2 = 0.01,\ 0.05,\ 0.09$, individually. It is easy to verify that all conditions of Theorem 1 are satisfied under these three circumstances. Figs.3-5 show the evolution process of the amplitude maps which describe three competitors population distribution characteristics at different instants $t = 20,\ 30,\ 40,\ 50,\ 60,\ 70,\ 80,\ 90,\ 100$ while $d_2 = 0.01,\ 0.05,\ 0.09$, respectively. When $d_2 = 0.01$, with the increase of time t, the population density amplitude maps of competitors in different regions demonstrate irregular jumping, and the oscillation amplitude is larger. When $d_2 = 0.05$, with the increase of time t, the oscillation amplitude of the population density of competitors in different regions gradually decreases, and gradually presents a regular fluctuation. When $d_2 = 0.09$, with the increase of time t, the population amplitude graph of competitors in different regions presents a state similar to a straight line, and floats up and down near the non-trivial equilibrium point in this state.



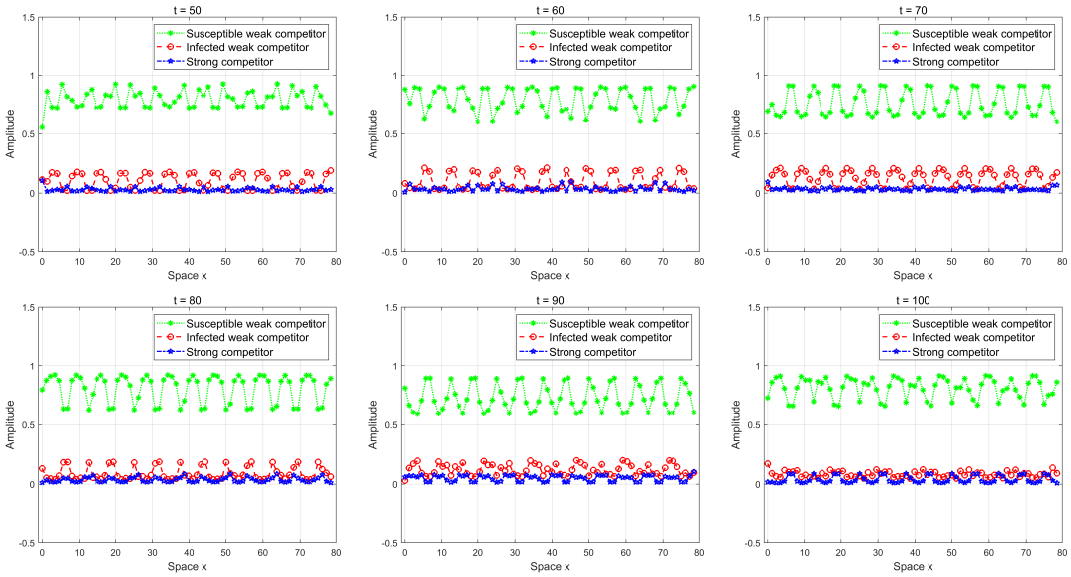


Figure 3. Amplitude maps of the time evolution of three competitors at different instants $t = 20,\ 30,\ 40,\ 50,\ 60,\ 70,\ 80,\ 90,\ 100$, and the initial conditions are $(0.8003 + 0.01cos(x),\ 0.1046 + 0.01cos(x),\ 0.0564 + 0.01cos(x))$. The diffusivities are $d_1 = -0.01,\ d_2 = 0.01,\ d_3 = 0.01$. The other parameters of network (1) are listed in Table 2.

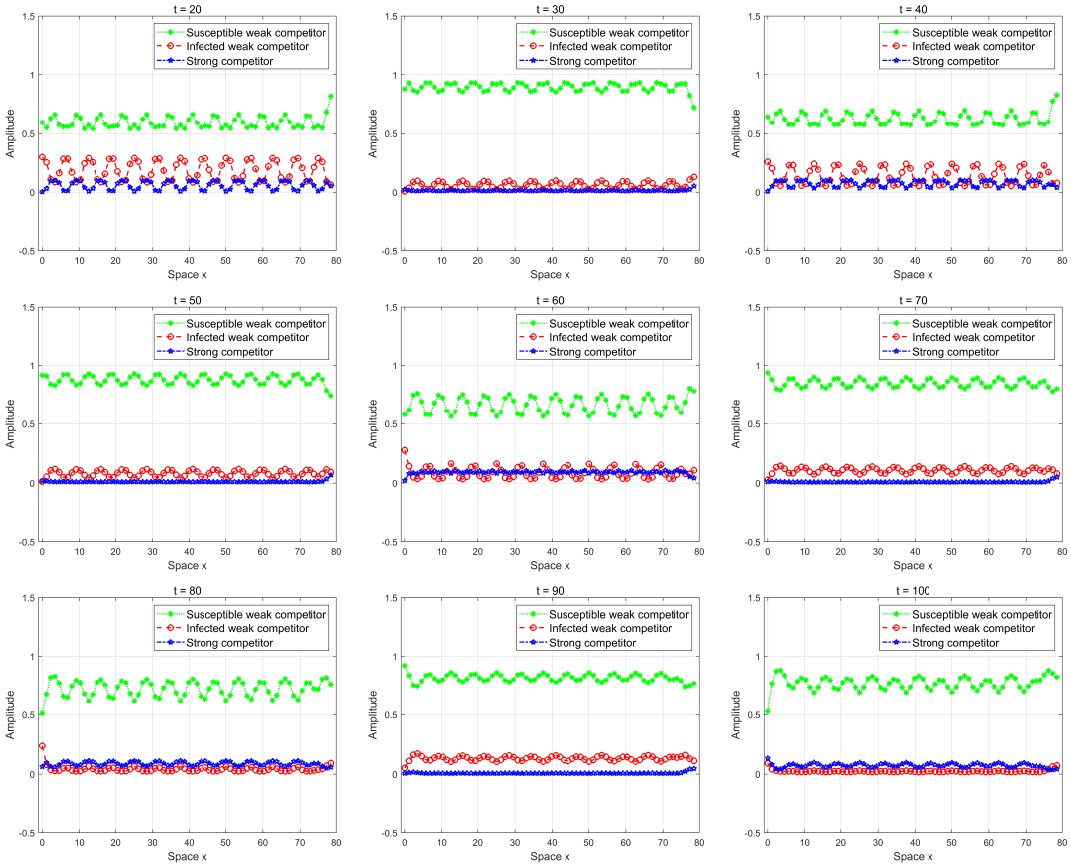


Figure 4. Amplitude maps of the time evolution of three competitors at different instants $t = 20,\ 30,\ 40,\ 50,\ 60,\ 70,\ 80,\ 90,\ 100$, and the initial conditions are $(0.8003 + 0.01cos(x),\ 0.1046 + 0.01cos(x),\ 0.0564 + 0.01cos(x))$. The diffusivities are $d_1 = -0.01,\ d_2 = 0.05,\ d_3 = 0.01$. The other parameters of network (1) are listed in Table 2.

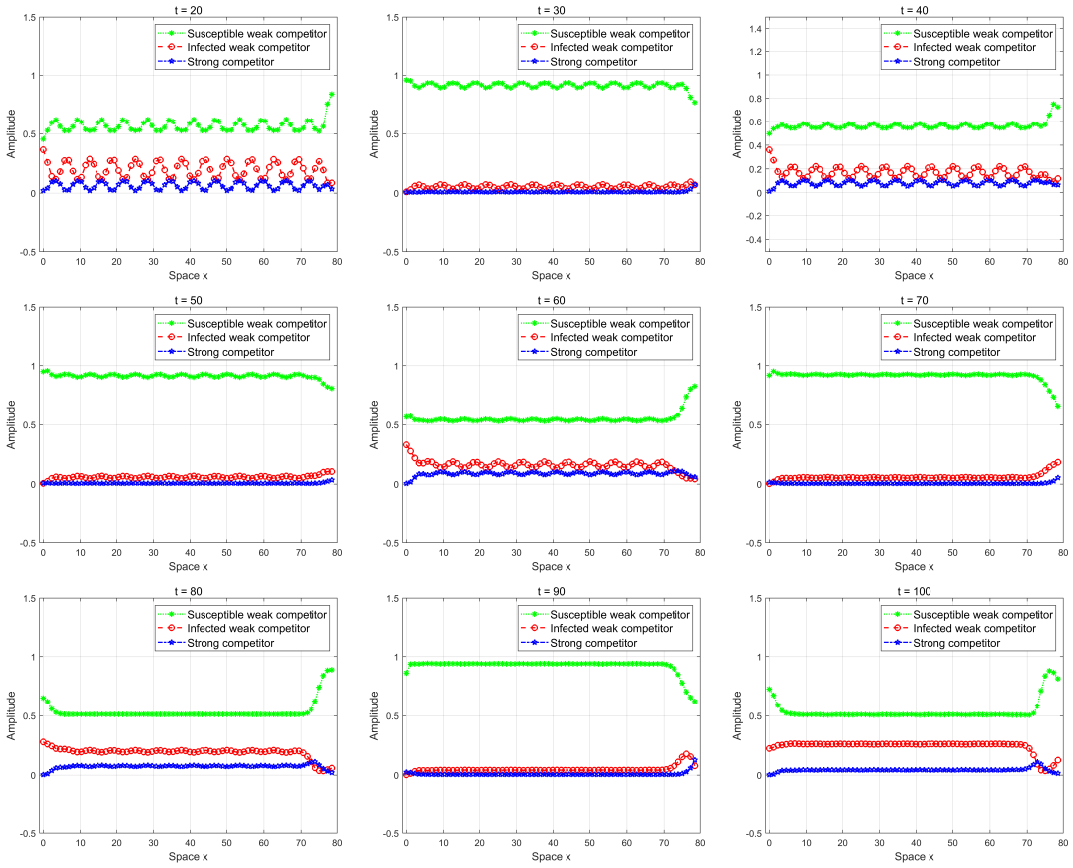


Figure 5. Amplitude maps of the time evolution of three competitors at different instants $t = 20,\ 30,\ 40,\ 50,\ 60,\ 70,\ 80,\ 90,\ 100$, and the initial conditions are $(0.8003 + 0.01cos(x),\ 0.1046 + 0.01cos(x),\ 0.0564 + 0.01cos(x))$. The diffusivities are $d_1 = -0.01,\ d_2 = 0.09,\ d_3 = 0.01$. The other parameters of network (1) are listed in Table 2.

In the light of Figs.3-5, we plot spatiotemporal wave diagrams and one-dimensional patterns of network (1) at instant $t = 100$ while $d_2 = 0.01,\ 0.05,\ 0.09$, respectively. When $d_2 = 0.01$, network (1) ultimately emerges periodic discontinuous zigzag patterns. As d_2 gradually increases to 0.05, the discontinuous zigzag patterns tardily becomes continuous. When d_2 increases to 0.09 with time t increases, network (1) embodies periodic stripe patterns.

Remark 6. *The positive self-diffusion coefficient represents species transfer from high-density regions to low-density regions. However, in nature, weak herbivores will adopt gregarious behaviors, which will lead to the transfer of species from low-density areas to high-density areas. Therefore, in network (1), we choose the self-diffusion coefficient d_1 of the susceptible weak competitor as a negative value, so as to be more realistic.*

Remark 7. *(Figs.6-8 Biological Interpretation). As can be seen from these figures, when the velocity of diffusivity d_2 of the susceptible weak competitor in network (1) is high, the density distribution of each competitor will appear as a striped pattern. The pattern of the infected weak competitor was basically consistent with the pattern of the strong competitor. The high-density pattern of the susceptible weak competitor matches the low-density pattern of the strong competitor. It is indicated that strong competitors are more likely to prey on susceptible weak competitors, and susceptible competitors tend to move away from high-density areas of strong competitors.*

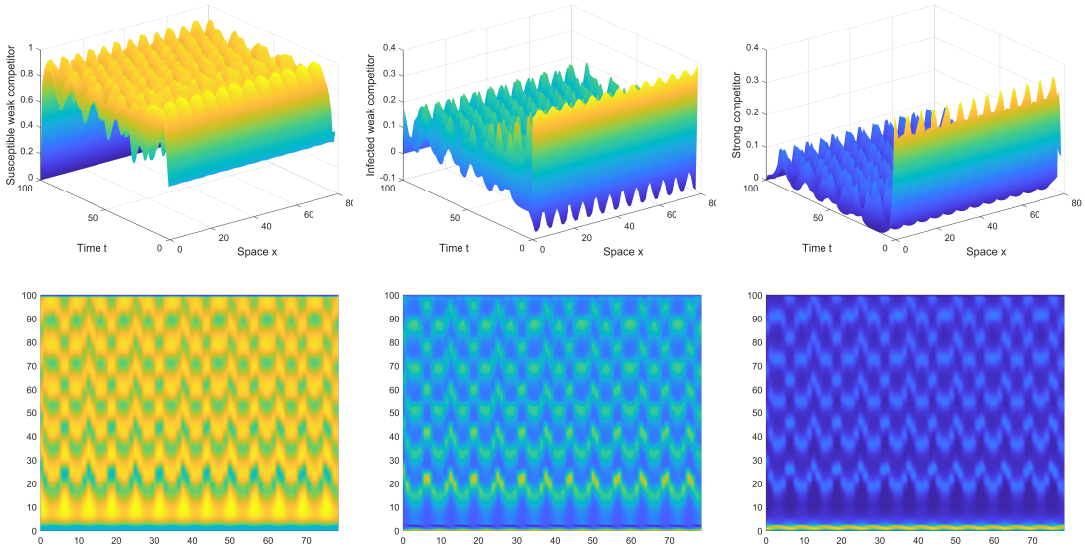


Figure 6. Spatiotemporal wave diagrams and one-dimensional patterns of three competitors at instant $t = 100$, and the initial conditions are $(0.8003 + 0.01cos(x),\ 0.1046 + 0.01cos(x),\ 0.0564 + 0.01cos(x))$. The diffusivities are $d_1 = -0.01,\ d_2 = 0.01,\ d_3 = 0.01$. The other parameters of network (1) are listed in Table 2.

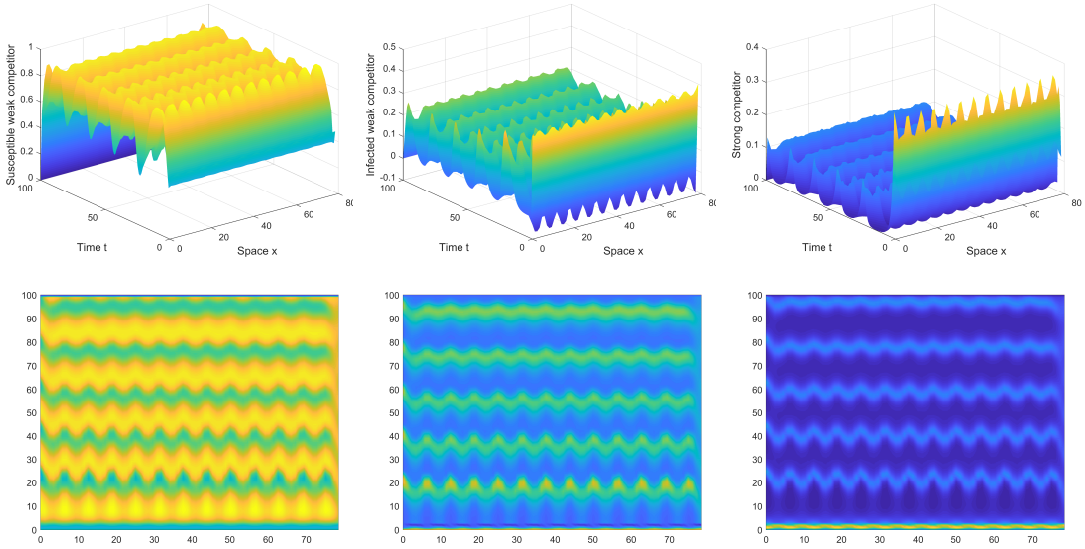
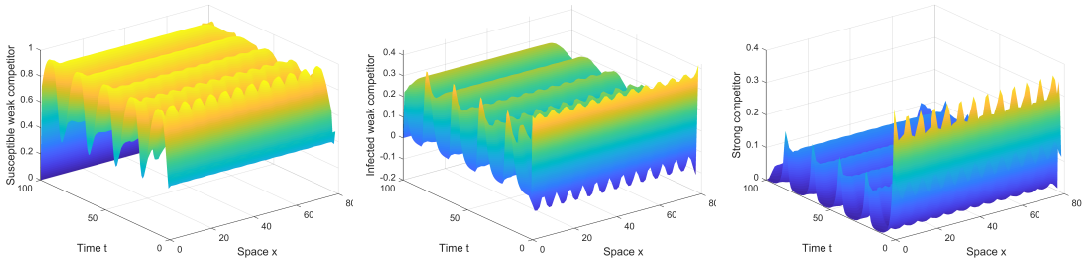


Figure 7. Spatiotemporal wave diagrams and one-dimensional patterns of three competitors at instant $t = 100$, and the initial conditions are $(0.8003 + 0.01cos(x),\ 0.1046 + 0.01cos(x),\ 0.0564 + 0.01cos(x))$. The diffusivities are $d_1 = -0.01,\ d_2 = 0.05,\ d_3 = 0.01$. The other parametes of network (1) are listed in Table 2.



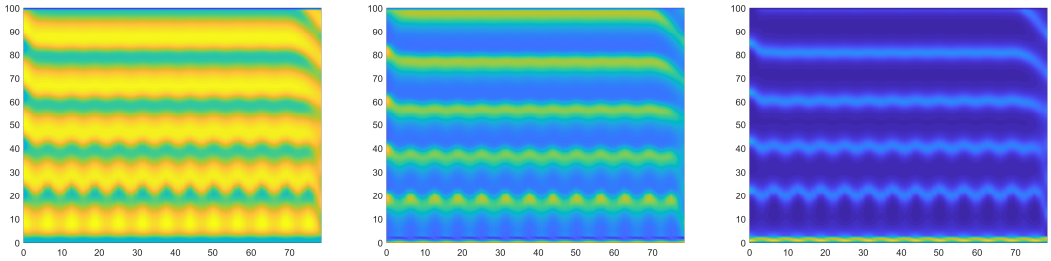


Figure 8. Spatiotemporal wave diagrams and one-dimensional patterns of three competitors at instant $t = 100$, and the initial conditions are $(0.8003 + 0.01cos(x),\ 0.1046 + 0.01cos(x),\ 0.0564 + 0.01cos(x))$. The diffusivities are $d_1 = -0.01,\ d_2 = 0.09,\ d_3 = 0.01$. The other parameters of network (1) are listed in Table 2.

5.2. **Impact of incubation delay τ on the Hopf bifurcation.** In this subsection, we show the temporal solutions and phase portraits of network (1) influenced by incubation delay τ. We set up $d_1 = 1,\ d_2 = 1,\ d_3 = 1,\ d = 0.4,\ \alpha = 0.4,\ p_1 = 0.72$, and the rest of the parameters remain constant as listed in Table 2. We study network (1) with spatial scale $\Omega = (0, 25\pi)$ and temporal scale $t = (0, 300)$ under the homogeneous the Neumann boundary conditions, and the initial conditions are $(0.7, 0.2, 0.01)$.

Clearly, all conditions of Theorem 2 and 3 hold exact. By calculation of (9), (11) and (12), we have $\omega_0 = 0.1661$ and there exists a positive minimum constant $\tau_0 = 3.4482$ such that the non-trivial equilibrium point E^* of network (1) is unstable if $\tau \in [0, \tau_0)$ and is stable if $\tau > \tau_0$. Further, network (1) undergoes a the Hopf bifurcation at the non-trivial equilibrium point E^* when $\tau = \tau_0$. Numerical simulation illustrates the achievements above (see Figs.9-10. When $\tau = \tau_0$, we have $c_1(0) = 3.6329 - 17.739i$, it follows from (18) that $\mu_2 = 0.0083673 > 0$ and $\beta_2 = 7.2658 > 0$. Therefore, the bifurcation occurs when τ crosses $\tau = 0$ to the right $(\tau > \tau_0)$, and the corresponding periodic orbits are unstable.

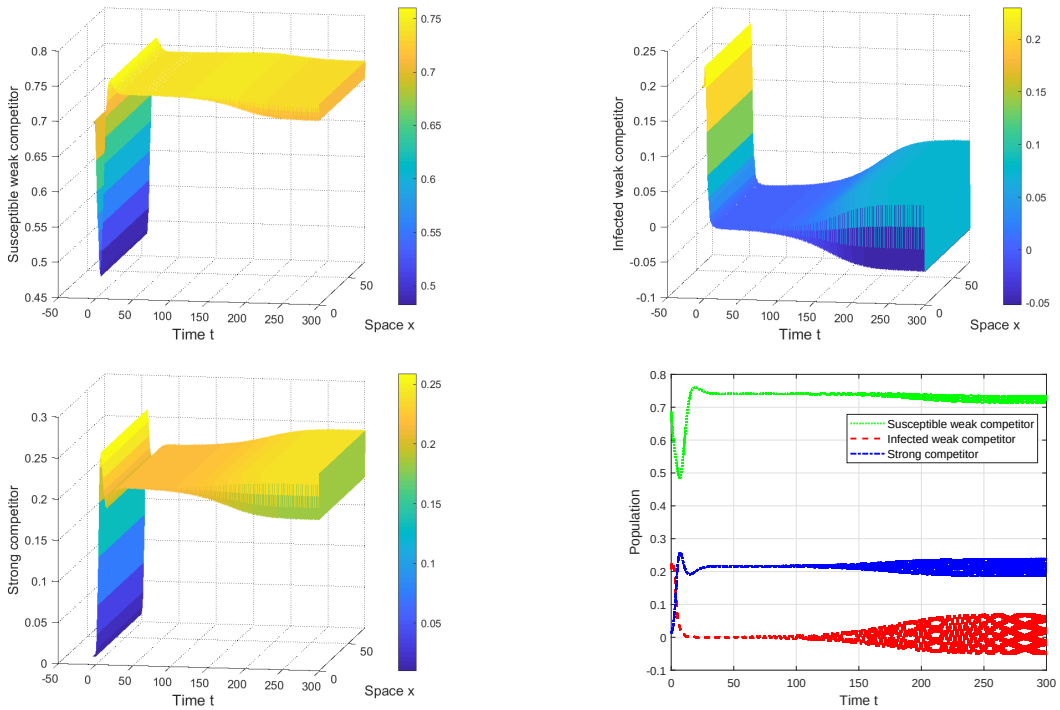


Figure 9. Temporal solutions and phase portraits of network (1) of network (1) under the Neumann boundary conditions, and the initial conditions are $(0.7,\ 0.2,\ 0.01)$ with $\tau = 3.4 < \tau_0 = 3.4482$. The diffusivities are

$d_1 = 1,\ d_2 = 1,\ d_3 = 1$. The parameters values are $p_1 = 0.72,\ d = 0.4,\ \alpha = 0.4$, and the other parameters of network (1) are listed in Table 2.

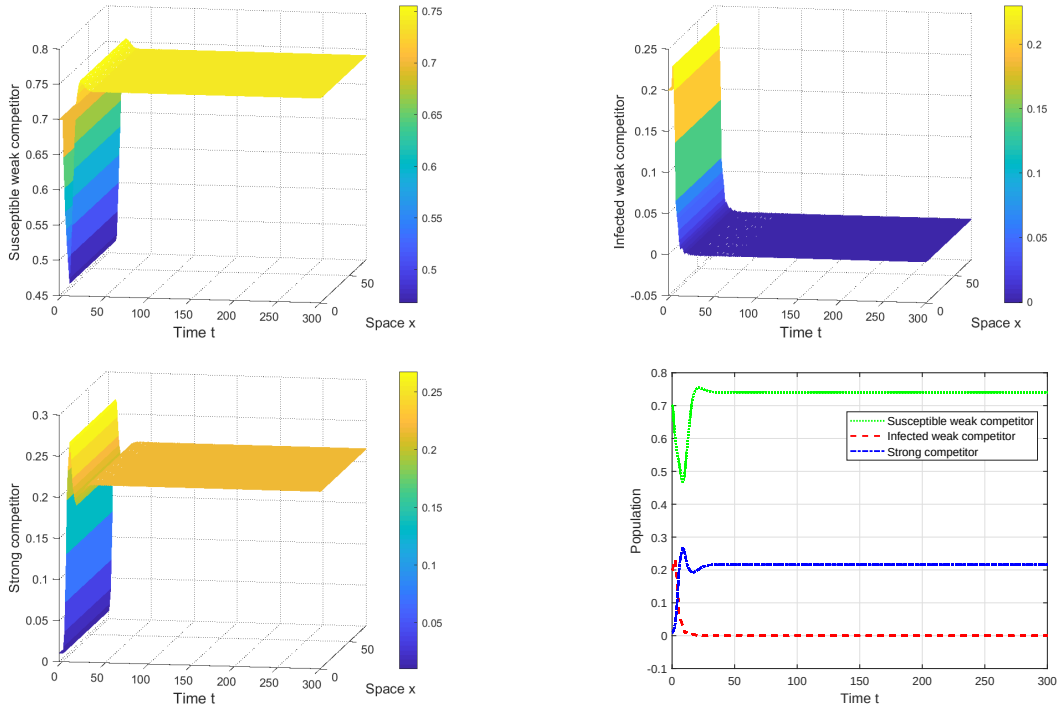


Figure 10. Temporal solutions and phase portraits of network (1) of network (1) under the Neumann boundary conditions, and the initial conditions are $(0.7,\ 0.2,\ 0.01)$ with $\tau = 3.5 > \tau_0 = 3.4482$. The diffusivities are $d_1 = 1,\ d_2 = 1,\ d_3 = 1$. The parameters values are $p_1 = 0.72,\ d = 0.4,\ \alpha = 0.4$, and the other parameters of network (1) are listed in Table 2.

Remark 8. *As the incubation of the epidemic increases slightly, the population density of network (1) become temporarily stable. But in the latent period of infectious disease, the virus still has a certain infectivity, so are more likely to infect other populations. However, with the further increase of the incubation period of the epidemic, the greater the risk, the population density of network (1) will reappear to a original state of oscillation.*

6. Conclusion

In this paper, an eco-epidemiological competition network with diffusion and delay is put forward. Through analyzing the characteristic equations located by continuous one-dimensional positions, we separately explore the impressions of diffusion coefficient and incubation time delay on the sudden change of network dynamic characteristics. The research results indicate that the patterns caused by the Turing instability transform from discontinuous zigzag to continuous zigzag, and finally evolve into stripe as the diffusion coefficient of infected weak competitor increases with no time delay in the network. Simultaneously, it is discovered that with the increase of incubation time delay, the dynamic behavior of the network changes abruptly, and the originally unstable oscillation period solution will converge to the non-trivial equilibrium point. Last but not least, the stability and direction of the Hopf bifurcation are also determined via the normal form theory and the center manifold reduction theory.

The location information involved in a delayed eco-epidemiological competition network proposed is one-dimensional, and the pattern formed is periodic zigzag or strip, the specific spatial

the Turing pattern cannot be obtained, nonetheless. In the future, we will take more location information into the follow-up consideration to characterize the specific spatial the Turing patterns.

7. Acknowledgment

This work is supported in part by the National Natural Science Foundation of China under Grant 62073172, the Natural Science Foundation of Jiangsu Province of China under Grant BK20221329, and the Open Research Project of the State Key Laboratory of Industrial Control Technology of Zhejiang University under Grant ICT2022B43.

References

[1] Abbasov, A.M., Mamedov, Z.F., Tvaronaviciene, M., Borodin, A., Vygodchikova, I.Y., Aliev, A.A. Estimation and prediction dynamics of the spread of the coronavirus infection using minimax approximation criterion and polynomial splines, *Appl. Comput. Math.*, V.21, N.1, 2022, pp.78-100.

[2] Ambika, G., Kurths, J. Tipping in complex systems: theory, methods and applications, *Eur. Phys. J. Spec. Top.*, V.230, N.16-17, 2021, pp.3177-3179.

[3] Bentout, S., Djilali, S., Touaoula, T.M., Zed, A., Atangana, A. Bifurcation analysis for a double age dependence epidemic model with two delays, *Nonlinear Dynam.*, V.108, N.2, 2022, pp.1821-1835.

[4] Bhaskar, C., Santu, G., Nandadulal, B. Reaction-diffusion predator-prey-parasite system and spatiotemporal complexity, *Appl. Math. Comput.*, V.386, 2020, Art. no.125518.

[5] Bojkva, D., Klann, K., Koch, B., Widera, M., Krause, D., Ciesek, S., Cinatl, J., Munch, C. Proteomics of SARS-CoV-2-infected host cells reveals therapy targets, *Nature*, V.583, N.7816, 2020, pp.469-472.

[6] Cai, L.M., Liu, J.L., Chen, Y.M. Dynamics of an age-structured HIV model with super-infection, *Appl. Comput. Math.*, V.20, N.2, 2021, pp.257-276.

[7] Castellazzo, A., Mauro, A., Volpe, C., Venturino, E. Do demographic and disease structures affect the recurrence of epidemics?, *Math. Model. Nat. Pheno.*, V.7, N.3, 2012, pp.28-39.

[8] Chakraborty, B., Ghorai, S., Bairagi, N. Reaction-diffusion predator-prey-parasite system and spatiotemporal complexity, *Appl. Math. Comput.*, V.386, 2020, Art. no.125518.

[9] Chesson, P.L., Ellner, S. Invasibility and stochastic boundedness in monotonic competition models, *J. Math. Biol.*, V.27, N.2, 1989, pp.117-138.

[10] Dai, H., Liu, Y.Y., Wei, J.J. Stability analysis and the Hopf bifurcation in a diffusive epidemic model with two delays, *Math. Biosci. Eng.*, V.17, N.4, 2020, pp.4127-4146.

[11] Dai, W.H., Zhang, B., Jiang, X.M., Su, H.X., Zhao, Y., Xie, X., Jin, Z.M., Peng, J.J., et al. Structure-based design of antiviral drug candidates targeting the SARS-CoV-2 main protease, *Science*, V.368, N.6497, 2020, pp.1331-1335.

[12] Garg, H., Kaur, G. Algorithms for screening travelers during Covid-19 outbreak using probabilistic dual hesitant values based on bipartite graph theory, *Appl. Comput. Math.*, V.20, N.1, 2021, pp.22-48.

[13] Garvie, M.R. Finite-Diffference schemes for reaction-diffusion equations modelling predator-prey interactions in MATLAB, *Bull. Math. Biol.*, V.69, 2007, pp.931-956.

[14] Grziwotz, F., Chang, C.W., Dakos, V., van Nes, E.H., Schwarzlander, M., Kamps, O., Hessler, M., Tokuda, I.T., et al. Anticipating the occurrence and type of critical transitions., *Sci. Adv.*, V.9, N.1, 2023, Art. no.eabq4558.

[15] Hassard, B.D., Kazarinoff, N.D., Wan, Y.H. *Theory and Application of the Hopf Bifurcation*, Cambridge University Press, Cambridge, 1981.

[16] Hu, G.P., Li, X.L. Stability and the Hopf bifurcation for a delayed predator-prey model with diease in the prey, *Chaos Soliton. Fract.*, V.45, N.3, 2012, pp.229-237.

[17] Huang, C.D., Cao, J.D, Xiao, M., Alsaedi, A., Alsaadi, F. Control bifurcation in a delayed fractional predator-prey system with incommensurate orders, *Appl. Math. Comput.*, V.293, 2017, pp.293-310.

[18] Ibragimov, A., Peace, A. Light driven interactions in spatial predator-prey chemotaxis model in the presence of chemical agent, *TWMS J. Pure Appl. Math.*, V.13, N.2, 2022, pp.222-244.

[19] Liu, J. Bifurcation analysis for a delayed SEIR epidemic model with saturated incidence and saturated treatment function, *J. Biol. Dynam.*, V.13, N.1, 2019, pp.461-480.

[20] Lotka, A.J. *Elements of Physical Biology*, Williams & Wilkins, Baltimore, 1925.

[21] Lu, Y.X, Xiao, M., Liang, J.L., Ding, J., Zhou, Y., Wan, Y.H., Fan, C.X. Hybrid control synthesis for the Turing instability and the Hopf bifurcation of marine planktonic ecosystems with diffusion, *IEEE Access*, V.9, 2021, pp.111326-111335.

[22] Murali, K., Sinha, S., Kohar, V., Ditto, W.L. Harnessing tipping points for logic operations, *Eur. Phys. J. Spec. Top.*, V.230, N.16-17, 2021, pp.3403-3409.
[23] Oqielat, M.N., Eriqat, T., Al-Zhour, Z., El-Ajou, A., Momani, S. Numerical solutions of time-fractional nonlinear water wave partial differential equation via Caputo fractional derivative: An effective analytical method and some applications, *Appl. Comput. Math.*, V.21, N.2, 2022, pp.207-222.
[24] Pavithran, I., Unni, V.R., Sujith, R.I. Critical transitions and their early warning signals in thermoacoustic systems, *Eur. Phys. J. Spec. Top.*, V.230, N.16-17, 2021, pp.3411-3432.
[25] Rietkerk, M., Bastiaansen, R., Banerjee, S., van de Koppel, J., Baudena, M., Doelman, A. Evasion of tipping in complex systems through spatial pattern formation, *Science*, V.374, N.6564, 2021, Art. no.eabj0359.
[26] Rudziva, M., Noreldin, O.A.I., Sibanda, P., Goqo, S.P. A bifurcation analysis of multicomponent convection in a rotating low prandtl number fluid with internal heating, *Appl. Comput. Math.*, V.21, N.1, 2022, pp.78-100.
[27] Tang, X.S., Li, J.Z. Chemotaxis induced the Turing bifurcation in a partly diffusive bacterial and viral diseases propagation model, *Appl. Math. Lett.*, V.100, 2020, Art. no.106037.
[28] Upadhyay, R.K., Roy, P., Rai, V. Deciphering dynamics of epidemic spread: The case of influenza virus, *Int. J. Bifurcat. Chaos*, V.24, N.5, 2014, Art. no.1450064.
[29] Volterra, V. Fluctuations in the abundance of a species considered mathematically, *Nature*, V.118, N.2972, 1926, pp.558-560.
[30] Wang, H., Zheng, X.C. Wellposedness and regularity of the variable-order time-fractional diffusion equations, *J. Math. Anal. Appl.*, V.475, N.2, 2019, pp.1778-1802.
[31] Wang, X.H., Wang, Z., Xia, J.W. Stability and bifurcation control of a delayed fractional-order eco-epidemiological model with incommensurate orders, *J. Frankl. Inst.*, V.356, N.15, 2019, pp.8278-8295.
[32] WHO. *Responding to the Avian Influenza Pandemic Threat: Recommended Strategic Actions*, World Health Organization, Geneva, 2005.
[33] Xu, C.J., Liao, M.X. Bifurcation analysis of an autonomous epidemic predator-prey model with delay, *Ann. Mat. Pur. Appl.*, V.193, N.1, 2014, pp.23-38.
[34] Zhao, L., Wang, Z.C., Ruan, S. Dynamics of a time-periodic two-strain SIS epidemic model with diffusion and latent period, *Nonlinear Anal. Real. World Appl.*, V.51, 2020, Art. no.102966.



Yunxiang Lu - received the B.S. degree from the College of Electrical Engineering, Tongda College of Nanjing University of Posts and Telecommunications, China, in 2019. He is currently pursuing the Ph.D. degree with the College of Automation and College of Artificial Intelligence, Nanjing University of Posts and Telecommunications, Nanjing, China. His current research interests include the neural dynamics, reaction diffusion systems, tipping and control, and eco-epidemiological competition systems.



Min Xiao - received the B.S. degree in Mathematics and the M.S. degree in Fundamental Mathematics from Nanjing Normal University, Nanjing, China, in 1998 and 2001, respectively, and the Ph.D. degree in Applied Mathematics from Southeast University, Nanjing, China, in 2007. He was a Post-Doctoral Researcher or a Visiting Researcher with Southeast University, the City University of Hong Kong, Hong Kong, and Western Sydney University, Sydney, NSW, Australia. He is currently a Professor with the College of Automation and College of Artificial Intelligence, Nanjing University of Posts and Telecommunications, Nanjing, China. His current research interests include information security, anomalous diffusion systems, networked control systems, tipping and control, and cyber-physical systems.



Jiajin He - received the B.S. degree from the College of Automation and College of Artificial Intelligence, Nanjing University of Posts and Telecommunications, Nanjing, China, in 2020, where he is currently pursuing the Ph.D. degree. His current research interests include anomalous diffusion systems, neural networks and bifurcation control.



Xiangyu Du - received the B.S. degree from the College of Automation and College of Artificial Intelligence, Nanjing University of Posts and Telecommunications, Nanjing, China, in 2021, where he is currently pursuing the Ph.D. degree. His current research interests include reaction-diffusion neural network, neural network optimal control and the Turing pattern.